A SIMPLE BIOSPHERE (SiB) MODEL FOR USE WITHIN GENERAL CIRCULATIONS MODELS: AN OVERVIEW OF THE MODEL DESIGN AND SOME PRELIMINARY RESULTS

P.J. Sellers
Department of Meteorology
University of Maryland
College Park, Maryland, U.S.A.

ABSTRACT

The importance of some of the interactions between the land surface and the atmosphere is discussed and the history of land surface-atmosphere modeling is briefly reviewed. The various representations of land surface processes used within General Circulation Models of the atmosphere (GCMs) to date are thought to be unrealistic and can provide little more than qualitative indications of the sensitivity of the atmospheric circulation to variations in the land surface condition. Recent work by Dickinson (1984) and Sellers et al. (1985) has approached the problem of modeling the vegetated land surface from a biophysical viewpoint with the aim of producing realistic but simple formulations for the description of interactions between the land surface and atmosphere. The Simple Biosphere (SiB) model of Sellers et al. (1985) is discussed as an example of this kind of approach. When coupled with a GCM, the model is designed to produce prognostic ground (ground cover and bare soil) and canopy vegetation temperatures, soil moisture content and fluxes of sensible and latent heat at every time step. Some tests of the performance of the model have been carried out at the local scale in isolation from a GCM and the sensitivity of the model to changes in the input parameters has been investigated. The possibility of using the physical state variables as calculated by the combined surface - atmosphere model with remotely sensed data for model initialization and validation is briefly discussed. Most of the material in this paper has been reproduced from Sellers et al. (1985) and Sellers (1985)b.

1. VEGETATION-CLIMATE INTERACTIONS

Until recently, little attention was paid to the effects of differing surface types upon local and regional climate; the vegetation (or lack of it) in a given region was assumed to be solely the result of climatic forcing with minimal feedback onto the climate itself (see Tivy; 1977, Walter; 1973).

Recent work has demonstrated, however, that the interactions between land surface and atmosphere are significant and complex. The land surface influences the atmosphere via three principal modes of exchange: radiation, momentum, and sensible and latent heat transfer. Early GCM experiments were performed to determine the extent of the sensitivity of the global and regional climate to changes in these fluxes. Often, these sensitivity experiments assumed drastic and unrealistic changes in the land surface properties by the simple alteration of a specific surface parameter; e.g., albedo, roughness length, soil moisture fraction, etc. However, the results of these early efforts showed that the different kinds and scales of surface-atmosphere interactions could have significant effects on the atmospheric circulation. Three of these experiments, concerned with radiative, heat and momentum transfer, respectively, serve as useful illustrations.

Charney (1975) hypothesized that the removal of vegetation in arid regions would increase the surface albedo, reduce the amount of radiation absorbed, lower the equivalent surface temperature and further promote subsiding motion in the overlying air mass. This chain of events (which assumes that any other processes influenced by the presence or absence of vegetation

are negligible) would act to maintain the area in a desert-like state. Simulations using GCMs with different prescribed surface albedos have qualitatively supported this thesis (see Charney et al; 1977 and Mintz; 1984).

Shukla and Mintz (1982) conducted a simple experiment with a General Circulation Model in which the land surface was assumed to be evaporating freely (first case) and completely dry (second case). The resultant fields of precipitation, air temperature and wind vector were found to be significantly different.

Sud and Smith (1985) conducted a numerical experiment wherein the roughness length assigned to the Sahara desert (usually taken to be 44 cm in their model, i.e., representative of a tall vegetation cover) was changed to a lower value of 0.2 mm, more realistic for bare sand. This change reduced the frictional drag on the boundary layer and moved the simulated rainfall band further south to a latitude more consistent with observations.

The paper of Mintz (1984) provides a general review of the history of such studies by summarizing the results of eleven experiments conducted with GCMs wherein the nature of the land surface parameterization (albedo, soil moisture, roughness length, etc.) was changed from a 'control' condition to a physically different state. The results obtained by different research groups using different GCMs were qualitatively similar in their predictions of the changes induced in the regional fields of air temperature, humidity, winds, pressure and precipitation for similar alterations in the drag, radiation absorption and energy partition properties of the land surface.

These studies all used relatively simple descriptions (see next section) of the various processes occurring at the land surface-atmosphere interface. More sophisticated and realistic models of the energy and mass balance of the vegetated land surface have been developed by a separate scientific community concerned with biophysics, agrometeorology and hydrometeorology. Generally, their studies were concerned with the local one-dimensional description of biophysical processes applicable to small areas.

A number of these studies used prescribed atmospheric conditions to drive Soil-Plant-Atmosphere Models (SPAMs) capable of simulating the effects of changing the vegetation type of an area. Sellers (1981) and Sellers and Lockwood (1981) demonstrated that the energy and water balance of a region could be highly dependent upon plant physiology and morphology: the former factor controls the transpiration rate while the latter has a marked effect on the annual interception loss rate (that proportion of rainfall that is held on plant leaves as liquid water and then re-evaporates to the atmosphere without reaching the bulk soil moisture store). Otterman (1981), Goudriaan (1977) and Ross (1975), who gives earlier references, have shown how plant structure affects the absorption of radiation in a region by the trapping of light in multiple reflections between plant elements.

These one-dimensional studies have simulated exchange processes in a biophysically realistic way, but most of them are far too elaborate and site-specific to be considered for implementation in a GCM. What is required is a generally applicable, realistic but simple representation of the biophysical elements that control such exchanges. In this paper I review the simpler models used up to now in GCMs, discuss their successes and short-comings, then briefly describe the Simple Biosphere

model of Sellers et al. (1985) as an example of the trend towards biophysically realistic formulations.

The Simple Biosphere model is intended to be as physically and biologically realistic as the constraints of computer resources allow. Initially, this model will be physiologically reactive to atmospheric conditions, but the type, density and health of the vegetation will be prescribed as functions of season and location. It should provide more realistic fields of sensible heat, latent heat and drag over the continents than do existing formulations, provided it is coupled to a GCM with an adequate simulation of the planetary boundary layer, distribution of rainfall and other climatic features.

Subsequent studies will explore the possibility of simulating growth and changes of vegetation interactively with the GCM, which will permit the simulation of the effects of atypical climatic conditions on the surface. If the goal of a truly interactive biosphere-atmosphere model were achieved, simulation studies of complex global problems would become feasible.

2. MODELING STRATEGIES

Three broad strategies are open to the would-be modeler of land-surface processes in GCMs. These are:

(i) the prescription of land surface parameters,

(ii) the use of conceptual models and

(iii) the use of biophysically-based models.

Until the work of Dickinson (1984), all GCM surface parameterizations had been confined to the first two approaches. (The sensitivity studies described in the preceding section all used such formulations.) The methodologies used in these approaches are summarized below.

2.1. Prescription of land surface parameters.

The global fields of terrestial albedo, roughness length and the Bowen ratio are specified and held constant for a given model run.

The equations describing the exchanges of radiation, momentum and heat are then given by:

Radiation

$$R_n = \int_0^\infty F_\ell \, (1 - \alpha_\ell) \cdot d\ell + \varepsilon_s F_t - \varepsilon_s \sigma T_s^4 \qquad (1)$$

R_n = net radiation absorbed by the land surface, W m^{-2}

F_ℓ = solar radiative flux density of wavelength ℓ , incident on the surface, W m^{-2}

α_ℓ = spectral albedo

ε_s = emissivity of the surface

σ = Stefan-Boltzman constant, W m^{-2} K^{-4}

T_s = surface radiative temperature, K

F_t = longwave flux downward from the atmosphere, W m^{-2}

Momentum

$$\vec{\tau} = \rho C_D |u_r| \vec{u}_r, \qquad (2a)$$

$\vec{\tau}$ = shear stress, kg m^{-1} s^{-2}

ρ = density of air, kg m^{-3}

C_D = surface drag coefficient

$\vec{u}_r$ = wind velocity at reference height z_r, m s^{-1}

$|u_r|$ = absolute value of $\vec{u}_r$, m s^{-1}

where C_D maybe either prescribed or obtained from

$$C_D = \frac{k}{\ln\left(\frac{z_r}{z_0}\right) - \phi_1}^2 \qquad (2b)$$

k = von Karman's constant, 0.41

z_r = reference height, m

z_0 = roughness length, m

ϕ_1 = non-neutral Paulson (1970) coefficient

All existing models prescribe fields of either C_D or z_0 and hold them constant over the annual cycle. Indeed, one constant value of z_0 is normally specified over the entire land surface. In the case of the GLAS (Goddard Laboratory for Atmospheric Sciences) GCM, this is 44 cm, representative of a tall forest cover (Sud and Smith, 1985).

Heat Fluxes

$$R_n - G = \lambda E + H \qquad (3a)$$

G = soil heat flux, W m^{-2}

E = evaporation rate, kg m^{-2} s^{-1}

λ = latent heat of vaporization, J kg^{-1}

H = sensible heat flux, W m^{-2}

$$B = \frac{H}{\lambda E} \qquad (3b)$$

B = Bowen ratio

$$G = C_g \frac{dT_s}{dt} \qquad (3c)$$

C_g = ground heat capacity, J m^{-2} K^{-1}

The processes described by (1) to (3) are shown in Figure (1). This equation set was used in the early GCMs with prescribed (sometimes seasonally varying) fields of the parameters α_ℓ , C_D or z_o, B and C_g. (Often, the ground heat flux term G was omitted by setting $C_g = 0.$) These surface parameterizations could be tuned to give acceptable results and were frequently used for sensitivity studies. However, the utility of the approach as a research tool is extremely limited because:

(i) no feedback effects (from climate to surface) can be simulated with prescribed surface properties; for example, the specification of a fixed Bowen ratio will yield an evaporative flux within an area even if the historical time integral of precipitation minus evaporation is large and negative in a region.

(ii) obtaining realistic climatological fields of the surface parameters necessitates an enormous data collection effort; in many regions, some of these quantities vary drastically from year to year.

2.2 Conceptual models.

Conceptual models were designed and implemented in an attempt to incorporate some of the feedback effects operating between the land surface and atmosphere and hence overcome the shortcomings of the 'prescribed field' approach described above. A review of these models is presented by Carson (1981), and so only a general outline of their common features is presented here.

Generally, the broad form of (1) to (3) were retained in these models, but the parameters in these equations were made to depend on the land surface

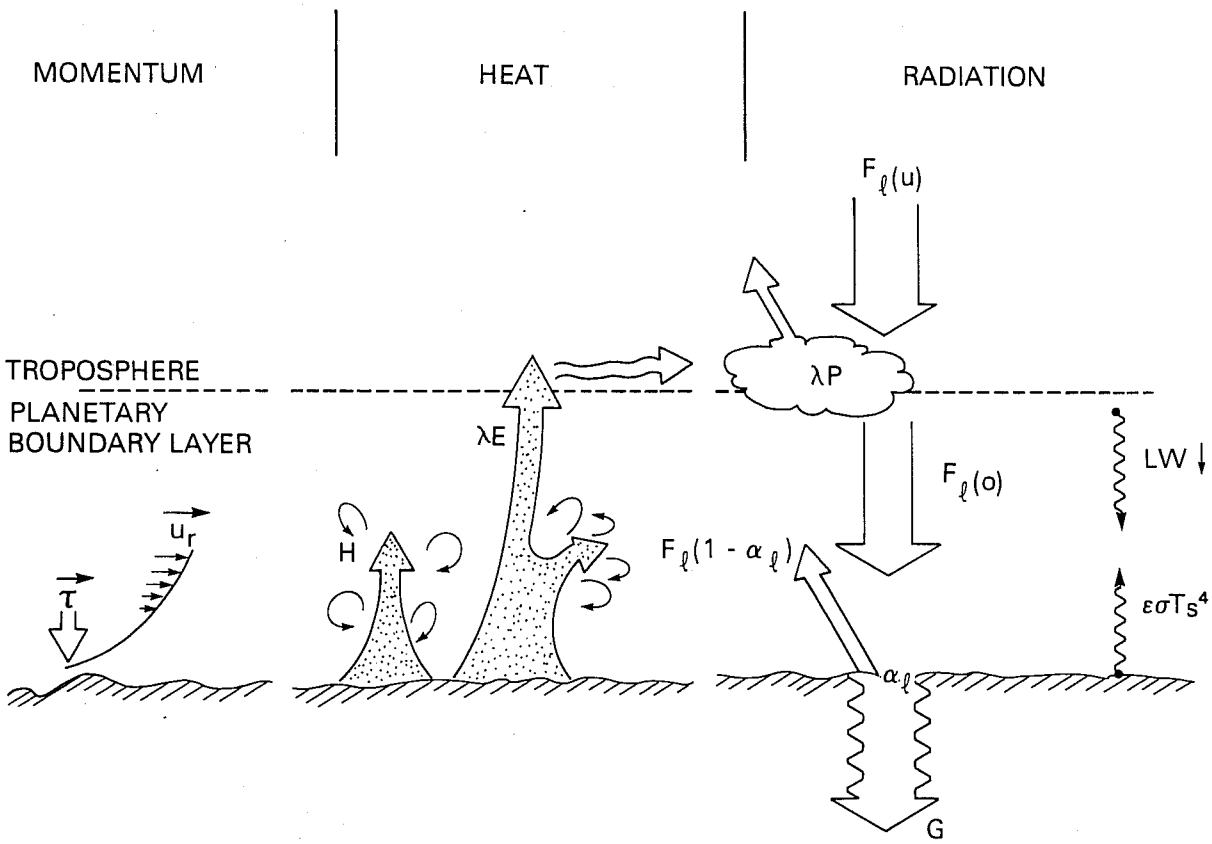

Fig. 1 Schematic diagram of interactions between the land surface and the atmosphere. The net radiation absorbed by the surface (R_n) is partitioned into storage, (G), sensible (H) and latent (λE) heat terms. The latent heat flux is released into the atmosphere upon condensation (λP). The resulting cloud cover may intercept and reflect significant amounts of the downcoming radiation

condition as predicted by the model, in particular, on the soil moisture storage. The soil moisture storage is usually represented as a 'bucket' which is filled by precipitation and emptied by evaporation and runoff. Most models define runoff as the surplus water produced when the bucket overflows (see Figure 2). Some surface hydrology models incorporate leakage terms to describe the runoff rate when the 'bucket' was less than full. The governing equation for the soil moisture wetness fraction, W, is:

$$\frac{dW}{dt} = \frac{1}{\theta_S D}\left[P - \frac{E}{\rho_W} - R_O\right] \qquad (4)$$

W = soil moisture wetness fraction

$= \theta/\theta_S$

θ = volumetric soil content, $m^3\ m^{-3}$

θ_S = value of θ at saturation, $m^3\ m^{-3}$

D = thickness of the hydrologically active soil layer, m

P = precipitation rate, $m\ s^{-1}$

ρ_W = density of water, $kg\ m^{-3}$

R_O = runoff rate, $m\ s^{-1}$

The maximum moisture storage of the soil is given by the product $\theta_S D$.

The addition of (4) to the set allows the modeler to specify some of the feedback effects explicitly in the surface formulation.

A few examples of such feedback effects are given below:

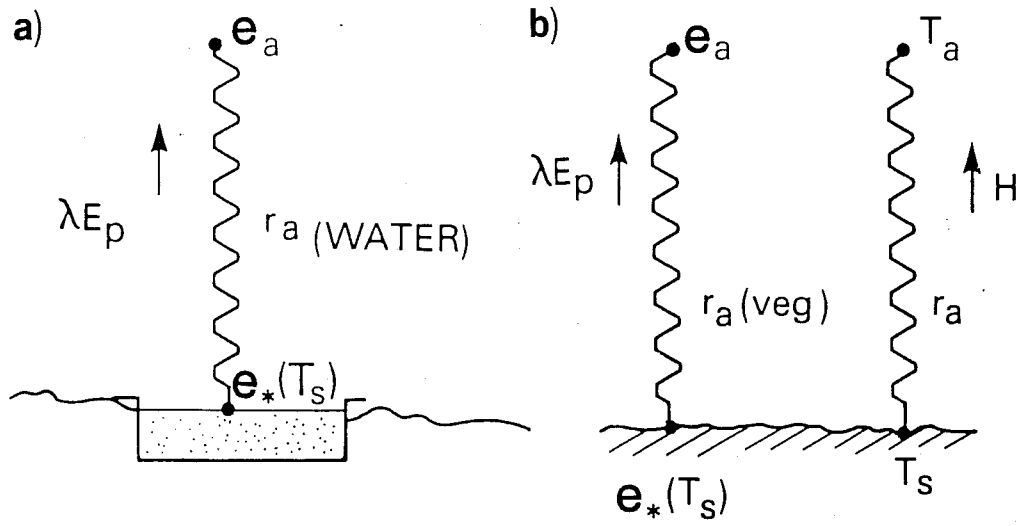

c) $B = f(W)$

$\lambda E = B.Ep$

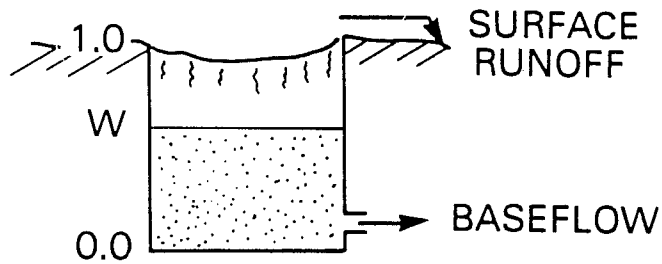

Fig.2 Surface hydrology as used in most contemporary GCMs. The resistance r_a between surface and air is indicated as in electric circuit theory. An estimate of evapotranspiration appropriate to either (a) an open water lysimeter or (b) a saturated surface with temperature T_s is used to calculate the 'potential evapotranspiration' rate. This quantity is then multiplied by a function of the soil moisture fraction, W, to account, along with runoff, for the depletion of soil moisture as sketched in (c).

Radiation

Surface albedo can be made a function of soil moisture, for example,

$$\alpha_{\ell} = 0.30 - 0.15\ W \qquad (5)$$

Carson and Sangster (1981) used (5) in a British Meteorological Office (MO) GCM simulation run and found it enhanced contrasts between wet and dry regions when compared to runs using prescribed albedos. Qualitatively, (5) is reasonable in that dead vegetation or bare ground is more reflective in the visible spectral region (0.4 - 0.7 μm) than is live vegetation, which absorbs this higher energy radiation for photosynthesis. Furthermore, the vegetation albedo may have a highly non-linear dependence on soil moisture content, related to the survival strategy of the dominant species in a region; for example, deciduous versus coniferous forests, opportunistic species (desert grasses) versus perennials (cacti).

Momentum

To the author's knowledge, no feedback effects on momentum transfer have ever been incorporated into a GCM simulation.

Latent Heat fluxes

The conceptual surface models yield their greatest improvement over the prescribed 'field approach' in the calculation of surface fluxes. The most common methodology is as follows: a potential evaporation rate is calculated using either

$$\lambda E_p = \frac{e*(T_s) - e_r}{r_a} \frac{\rho c_p}{\gamma} \qquad (6a)$$

or

$$\lambda E_p = \frac{\Delta(Rn - G) + [e*(T_r) - e_r]\,\rho c_p / r_a}{\Delta + \gamma} \qquad (6b)$$

E_p = potential evaporation rate, kg m^{-2} s^{-1}

$e*(T)$ = saturated vapor pressure at temperature T, mbars

e_r = vapor pressure at reference height, mbars

T_r = air temperature at reference height, K

c_p = specific heat of air, J kg^{-1}

Δ = slope of the saturation vapor pressure versus temperature curve, mbar K^{-1}

γ = psychrometric constant, mbar K^{-1}

r_a = aerodynamic resistance to the turbulent transfer of heat and vapor, s m^{-1}

r_a, the aerodynamic resistance to heat and vapor transfer between the source height (taken to be equivalent to the momentum sink height, z_o) and reference height, z_r, is calculated as the integral of the inverse of the transfer coefficient over the same distance. Thus:

$$r_a = \int_{z_o}^{z_r} \frac{1}{K_s}\, dz \qquad (6c)$$

K_s = vapor, heat transfer coefficient, m^2 s^{-1}

(6c) may be evaluated in terms of the wind speed at reference height, u_r, the roughness length, z_o, and two correction factors to allow for the effects of non-neutrality (see Paulson; 1970) as given in (6d) below

$$r_a \approx \frac{1}{k^2 u_r} \left[\ln\left(\frac{z_r}{z_o}\right) - \phi_1\right].\left[\ln\left(\frac{z_r}{z_o}\right) - \phi_2\right] \qquad (6d)$$

ϕ_2 = Paulson (1970) non-neutral correction factor for vapor transfer

The normal practice in the meteorological community is to combine the constant and non-neutral terms in (6d) to give a product of a drag coefficient, C_D, and a vapor/heat transfer coefficient, C_V.

$$r_a \simeq \frac{1}{C_D\, C_V\, u_r} \qquad (6d)$$

C_V = vapor or heat transfer coefficient

Equations (6) are modifications of the Penman (1948) expression for evaporation from an open-water surface. With appropriate values of r_a and $(R_n - G)$, the two formulae will yield identical results when applied to a surface completely covered with free water.

The potential evaporation rate given by (6) is usually adjusted for the limiting effects of soil moisture by

$$E = \beta\, E_p \qquad (7)$$

where β is a prescribed function of W, decreasing with decreasing W.

The combination of (6) and (7) would appear to place realistic bounds on the evaporation rate and also to describe its decline with soil moisture depletion in a reasonable way. In fact, neither assumption is correct.

First, if a value of the aerodynamic resistance, r_a, for an open-water surface is used (see figure 2a), both (6a) and (6b) will underestimate the evaporation rate from a saturated natural surface, which is almost always rougher. Use of the r_a value for open water gives an evaporation rate near that of a freely-ventilated surface covered with well-watered short

grass. (The evaporation rate for both surfaces is limited primarily by the amount of available energy, $R_n - G$.) Alternatively, if an r_a value appropriate to vegetation is used (i.e., with a z_o of the order of a few centimeters to meters), excessively large evaporation rates will be predicted (see Figure 2b), often exceeding the net radiation. While such a large rate would be typical of the evaporation rate from a wetted vegetation canopy, it will differ considerably from the transpiration rate of most natural surfaces, even when $W = 1$. Thus, the value of E_p given by (6) may be equal to that for either an open-water surface or for saturated canopy, but not of a freely-transpiring vegetation canopy.

The combination of (6) with (7) will yield different estimates of the evapotranspiration rate depending on whether one uses (6a) or (6b). In most GCMs, the surface temperature, T_s, is a prognostic variable. If (6a) is used with this value of T_s, the derived value of E_p will be too high in arid regions so that even when W is small, excessive evaporation is predicted. On the other hand, (6b) uses a surface temperature representative of an open-water lysimeter, which is different from the value of T_s carried by the model. The shortcomings of the (6a) and (7) combination have prompted many workers to use (6b) and (7) even though the predicted surface temperatures are then not consistent with evaporation rates. As Mintz (pers. comm.) says 'in nature, there are no telephonic connections between lysimeters and the rest of the land surface'.

More recently, the Penman-Monteith equation (see Monteith, 1973) has been used within a GCM. This modification of the original Penman (1948) formula defines the evapotranspiration rate from a vegetated surface in terms of a surface resistance, r_c, which is roughly equivalent to the resistance imposed by all the leaf stomata acting in parallel. Fig. 3 illustrates

the action of a stomatal pore.

$$\lambda E = \frac{\Delta\,(R_n - G) + \rho c_p\,(e*(T_r) - e_r)/r_a}{\Delta + \gamma\,(\frac{r_a + r_c}{r_a})} \qquad (8)$$

r_c = surface or canopy resistance, s m^{-1}

The use of (8) within a model is consistent with the prediction of a single prognostic ground temperature, T_s. Sud and Smith (1984) used this surface resistance formulation in a GCM along with a soil moisture term reducing the predicted evapotranspiration rate, thereby introducing an inconsistency similar to that produced by the combination of (6) and (7).

Equation (8) is a physically more acceptable description of the partition of energy at the surface than the combination of (6) and (7). One may obtain an understanding of the 'real' components of the β-function of (7) by combining (8) with (6b) (the commonly used expression for E_p) and expressing β as:

$$\beta = \frac{\Delta\,(R_n - G) + (e*(T_r) - e_r)\,\rho c_p/r_{a_1}}{\Delta\,(R_n - G) + (e*(T_r) - e_r)\,\rho c_p/r_{a_2}} \cdot \frac{\Delta + \gamma\,(r_{a_2} + r_c)/r_{a_2}}{\Delta + \gamma} \qquad (9)$$

r_{a_1} = assumed aerodynamic resistance for E_p calculation in (7), s m^{-1}

r_{a_2} = aerodynamic resistance for the vegetated surface, s m^{-1}

Equation (9) shows that if a value of r_a appropriate to the actual surface is used in (7), i.e. $r_{a_1} = r_{a_2}$, as opposed to the much higher value for

an open water surface which is usually used, the value of β is a function of r_a and r_c only. If instead the value of r_{a_1} is set to the original Penman 'open water' form then β depends on the values of all of the micrometeorological input variables $(R_n - G)$, T_r, and e_r and on r_{a_1}, r_{a_2} and r_c. The dependency of β on all of these variables as shown in (9) explains why attempts to fit β-functions to evapotranspiration data sets have produced less than satisfactory formulations.

In spite of the above failings, conceptual models can provide some accounting for the past accumulation of precipitation minus evaporation and runoff. Nevertheless, they are unreliable for the prediction of soil moisture, and the questionable physical significance of their various parameters discourages elaboration and experimentation beyond the crudest formulations. It is doubtful whether land-surface-change experiments conducted with such models give more than merely qualitative indications of the importance of various surface-related processes.

2.3 Biophysically-based Models

Both of the preceding methodologies specify the transfer of radiation, momentum and heat as independent processes, that is, the albedo, momentum and heat transfer coefficients and the soil hydrology formulations (if any) are presented as separate attributes of the land surface rather than as complementary facets of the vegetation-soil system. Since such models are limited as predictive tools a more fundamental approach to the problem is required. Ideally, the perfect model should be based entirely on biological and physical principles, but the limitations of current biophysical knowledge and the diversity of plant form and function to be found within a given region discourage such a stringent approach, and in any case such exactness would be too expensive in terms of computer resources. A more

realistic approach would be to base the model design upon biophysical principles and to attempt to capture the more important aspects of the biophysical controls over the surface-atmosphere exchanges. Although harder to design and implement than the two previous classes of model, a biophysical model may have the following benefits:

- it may be used to study more realistically the various feedback processes acting between the atmosphere and the vegetated surface.
- it offers a better prospect for the use of coupled surface-atmosphere models for prediction.
- the model may predict the values of physical state variables (rather than their conceptual analogues) for comparison with actual measurements and therefore allow model verification and initialization. In this respect, remotely-sensed data with global coverage and high temporal resolution may be immensely useful.

However, the complexity of any such proposed model is severely limited by the constraints of computer storage and operation. For the model to be 'simple without being trivial' and hence to satisfy computer storage, execution time, and vectorization constraints, it must also be capable of representing any land surface condition by an adjustment of its input parameters. With these constraints in mind, we should try to model radiation interception, momentum exchange and heat flux transfer as processes linked via the physical and biophysical properties of the vegetation cover. In pursuing this methodology, it is necessary to discard the view of plants as passive, damp surfaces evaporating at rates governed solely by the atmospheric demand and soil moisture condition. Rather, they are

living organisms which regulate the passage of water and gas through their systems in a highly efficient manner in order to maximize their prospects of growth and survival. If we are to understand the links between surface and atmosphere, we must introduce some of the influences of the physiology and morphology of the vegetation to be found in a given region.

The principal ways in which terrestrial plants may interact with the atmosphere are as follows:

i) Radiation: The chlorophyll molecule in green plants absorbs the visible, or photosynthetically active (0.4 - 0.7 μm), radiative flux energy in order to combine water and CO_2 into organic compounds needed for growth and maintenance; see figure 3. Green, healthy leaves are highly absorbent in this wavelength region (scattering coefficient $\leq$ 0.2) but weakly absorbent in the adjacent near infrared (0.7 - 3.0 μm) region (scattering coefficient of $\sim$ 0.8) where the lower energy radiation cannot drive photosynthesis. Bare ground on the other hand, usually exhibits a flatter scattering response with increasing wavelength with reflectances of about 0.1 to 0.3 over the spectral region 0.4 to 3.0 μm. The differing orientations of leaves within the canopy and the effect of multiple reflection and reinterception of radiation between the leaves makes the canopy an effective radiation trap within the visible region.

ii) Biophysical Control of Evapotranspiration: For CO_2 to reach the chlorophyll reaction sites, leaves must maintain an open pathway between the atmosphere and their saturated tissues and so inevitably lose water via evaporation over the same route (see figure 3). Higher plants control the amount of gas exchange (and hence water loss) by mean of valve-like structures on the leaf surface (stomata). Since only a small fraction of the radiant energy absorbed by leaves goes into photosynthesis or other

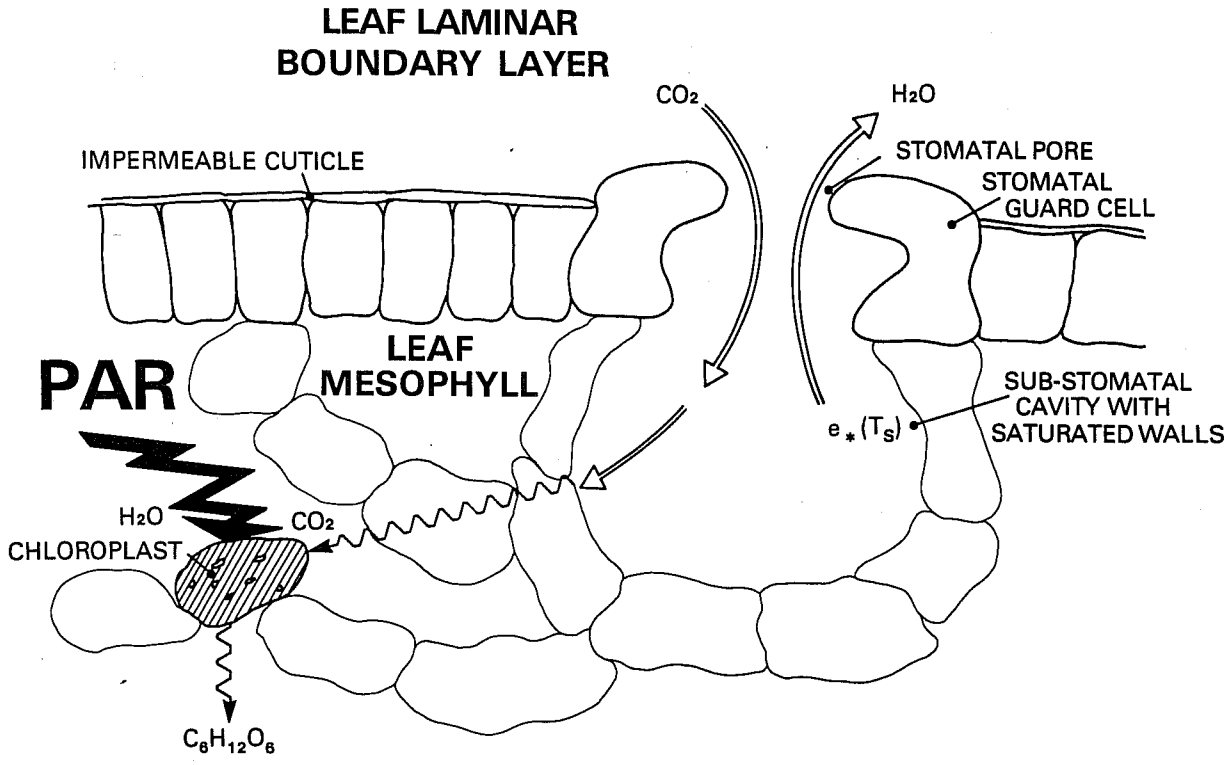

Fig.3 Processes of gas exchange and photosynthetically active radiation (PAR) interception at the leaf level. CO_2 diffuses in through the stomatal pore, the aperture of which is under active control. There is an inevitable loss of water vapour over the same route since the internal tissues are saturated. CO_2 and cellular water are combined into organic molecules in the mesophyll chloroplasts. These have chlorophyllous structures that are highly absorbent in the 0.4 - 0.7 µm spectral region.

storage terms, any decrease in the evaporation rate will be approximately balanced by a concomitant increase in the sensible heat loss.

iii) Momentum Transfer: Some plants grow tall in order to compete for light and, in some environments, to avoid being eaten by grazing animals. The vertically-extended canopy of tall vegetation presents a rough porous medium to the planetary boundary layer airflow when compared to short herbacious vegetation or bare soil. The resultant turbulence enhances the transport of sensible and latent heat away from the surface while exerting a drag force on the air mass.

iv) 'Insulation': The soil surface under a dense vegetation canopy intercepts less radiation and may also be aerodynamically sheltered. As a result, the net radiation available to the covered soil will be smaller and the component terms of the soil energy budget (evaporation, sensible heat and ground heat flux) will be correspondingly reduced.

The interactions described above are merely different manifestations of the same thing; optimal design of an integrated system (the plant) that can access and utilize various resources (radiation, soil moisture, CO_2, nutrients, etc.) in order to maximize the organism's chances of survival and growth. In modeling such a system we should take account of its linked integrated nature and represent the separate interactions in terms of a common self-consistent set of parameters. For example, the leaf area index alone influences the radiative transfer, momentum flux and energy partition properties of the vegetation in the SiB model.

3. THE STRUCTURE OF THE SIMPLE BIOSPHERE MODEL (SiB)

A schematic diagram of the Simple Biosphere Model (SiB) is shown in Figure 4. The land surface is represented by a vegetation canopy (upper

story) which may be separated from the soil surface by a 'trunk' space. The underlying soil surface may be bare or covered by ground vegetation and litter. Either or both of these vegetative layers may be continuous, broken or absent (e.g., as in tropical rainforest, savannah and desert, respectively). This structure may be adapted to crudely describe the morphological characteristics of the major vegetation formations (as defined by de Laubenfels, 1975 and Kuchler, 1949) by an adjustment of the heights, densities and cover fractions of the two vegetative layers. The parameters necessary for the operation of the model are obtained by classifying terrestrial biomes according to their vegetation, and assigning physical and physiological properties to each. This structure is the simplest method for providing the interactions summarized in the previous section.

The complete model uses boundary conditions set at a reference height, z_r, near the base of the lowest layer of the GCM to calculate dynamically the partition of energy at the surface. Of the seven prognostic variables in the SiB model, two are considered to undergo significant time rates of change over a model time step which may feed back onto the partition of energy. These are the canopy and ground temperatures, T_c and T_{gs}, which are directly associated with the 'fast' processes of radiation interception and partitioning into latent, sensible and storage heat terms. The remaining five prognostic variables are moisture stores: M_c and M_g are the amount of intercepted precipitation held as liquid of frozen water on leaves of the canopy or of the ground vegetation respectively, W_1 is the soil wetness fraction of the surface store, W_2 that of the root zone and W_3 that of the recharge zone. These 'slow' variables are updated between time steps since the feedback effects induced by their time rates of change on the 'fast' processes are taken to be negligible. Moisture stores change

their levels by the redistribution of water between themselves, by input from precipitation and by losses to runoff and evapotranspiration. The relegation of the five moisture stores to the status of accounting variables considerably simplifies the treatment of the surface energy balance. We now must use the initial state of the seven prognostic variables (see Table 1) in combination with the atmospheric forcing to calculate the time rates of change of the 'fast' variables T_c and T_{gs}, following which the values of the 'slow' variables may be updated.

In the model, the upper story and ground intercept, reflect and absorb the incoming radiation in accordance with the physical structure of the canopies and the optical properties of the plant elements and soil (Section 3.2). The absorbed energies, Rn_c and Rn_{gs}, are partitioned into latent, sensible and storage heat terms as shown below.

$$Rn_c = \lambda E_c + H_c + C_c \frac{dTc}{\partial t} \tag{10}$$

$$Rn_{gs} = \lambda E_{gs} + H_{gs} + C_{gs} \frac{dT_{gs}}{\partial t} \tag{11}$$

C_c, C_{gs} = effective heat capacity, J $K^{-1}m^{-2}$

T_c, T_{gs} = surface temperature, K

Rn_c, Rn_{gs} = net radiation absorbed, W m^{-2}

λE_c, λE_{gs} = latent heat fluxes, W m^{-2}

H_c, H_{gs} = sensible heat fluxes, W m^{-2}

The subscripts 'c' and '$_{gs}$' refer to the upper story canopy and ground (ground cover and soil) respectively. The terms in (10) and (11) are functions of (a) the prognostic variables--canopy temperature, ground

A: Prognostic Variables

T_c - canopy temperature, K

T_{gs} - ground temperature, K

M_c - liquid water stored on canopy foliage, m

M_g - liquid water stored on ground foliage, m

W_1 - soil moisture wetness fraction of surface store

W_2 - soil moisture wetness fraction of root zone

W_3 - soil moisture wetness fraction of recharge zone

B. Forcing Variables

F_o - incident radiative flux (spectral and angular components), W m^{-2}

P - precipitation, m s^{-1}

u_r - wind speed at reference height, m s^{-1}

T_r - air temperature at reference height, K

e_r - vapor pressure at reference height, mbar

C. Fluxes

Flux	Potential Difference	Resistances
H_c	$(T_c - T_a)\ \rho c_p$	$\overline{r_b}$
H_g	$(T_g - T_a)\ \rho c_p$	r_d
$H_c + H_g$	$(T_a - T_r)\ \rho c_p$	r_a
λE_c	$(e*(T_c) - e_a)\ \rho c_p/\gamma$	$f(\overline{r_{st}}, \overline{r_b}, M_c)$
λE_g	$(e*(T_g) - e_a)\ \rho c_p/\gamma$	$f(r_{surf}, r_g, r_d, M_g)$
$\lambda E_c + \lambda E_g$	$(e_a - e_r)\ \rho c_p/\gamma$	r_a

Where:

T_a, e_a = air temperature, vapor pressure in canopy air space; K, mbar

ρ, c_p = density, specific heat of air; kg m^{-3}, J kg^{-1} K^{-1}

γ = psychrometic constant, mbar K^{-1}

$\overline{r_b}$ = bulk boundary layer resistance, s m^{-1}

r_d = aerodynamic resistance between ground and canopy air space, s m^{-1}

r_a = aerodynamic resistance between canopy air space and reference height, s m^{-1}

$\overline{r_{st}}$ = bulk stomatal resistance of upper story vegetation, m s^{-1}

r_g = bulk stomatal resistance of ground vegetation, m s^{-1}

r_{surf} = bare soil surface resistance, s m^{-1}

$e*(T)$ = vapor pressure at temperature T, mbar

Table 1: Prognostic and forcing variables and variables associated with flux calculations in the SiB model.

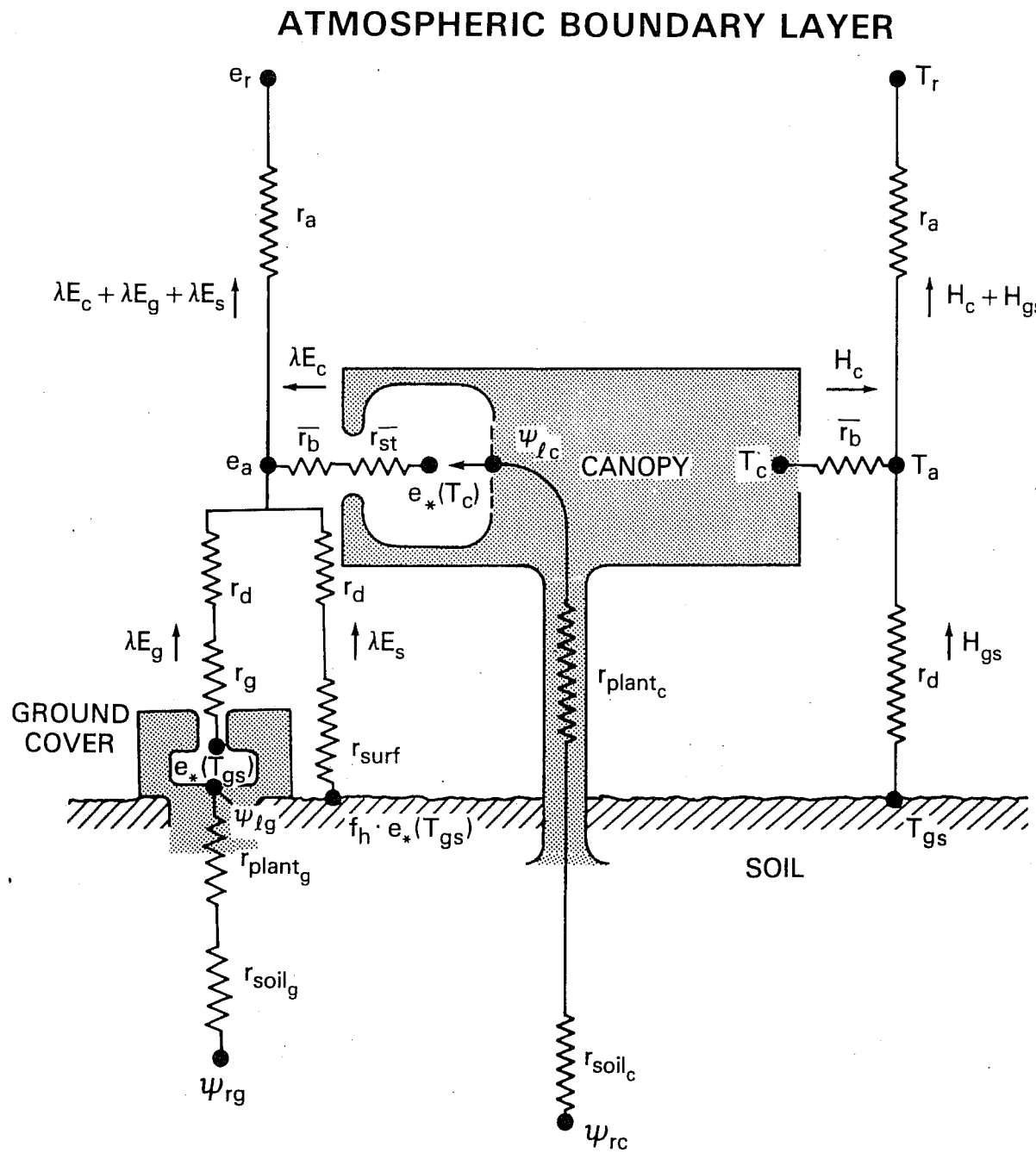

Fig.4. Framework of the Simple Biosphere (SiB) model. The transfer pathways for latent and sensible heat flux are shown on the left and right hand sides of the diagram respectively. Fluxes are proportional to differences in temperature T or water vapour pressure 'e' divided by the appropriate resistance. The subscript r refers to reference height, a to canopy air space, b to canopy element boundary layer, g to ground, d to air space between canopy and ground, and st to stomatal. Resistances are shown in terms of an analogous electrical circuit. These are defined in detail in Sections 3.3 and 3.4. The treatment of interception loss is excluded from this diagram for clarity.

temperature and the five moisture stores, (b) the boundary forcings of incoming radiation, precipitation, air temperature, humidity and wind speed at a reference height z_r, and, (c) six resistances: three aerodynamic resistances, r_a, r_b and r_d and three surface resistances, $\overline{r_{st}}$, r_g and r_{surf} (discussed in Section 3.4). Figure 4 illustrates the various resistances used in the SiB model.

The heat fluxes H_c, H_{gs}, λE_c and λE_{gs} are obtained from the above resistances and the differences between the surface (canopy or ground) and canopy air temperatures in the case of sensible heat and the corresponding differences in vapor pressure for the transfer of latent heat.

The resistances are equivalent to the integrals of inverse conductances per unit length over a specified length. In the cases of the aerodynamic resistances, r_a, $\overline{r_b}$ and r_d, the conductances correspond to the turbulent transfer coefficients for heat and vapor. The surface resistances $\overline{r_{st}}$ and r_g are the additional resistances to the transfer of vapor from the saturated tissues in the plants and r_{surf} is the equivalent resistance limiting the transfer of water from within the soil surface store to the air just above the soil. The aerodynamic resistances r_a, $\overline{r_b}$ and r_d are calculated from the morphology of the vegetated surface (see Section 3.3), the wind speed at reference height, u_r, and the temperature differences $(T_a - T_r)$, $(T_c - T_a)$ and $(T_{gs} - T_a)$ respectively. The surface resistances $\overline{r_{st}}$, r_g and r_{surf} are calculated from a combination of plant physiological and morphological parameters, incident radiation, temperature, vapor pressure and soil moisture. These calculations and the role of the canopy water stores M_c and M_g are reviewed in Section (3.4). The operation of the soil sub-model is explained in Section (3.5). A

full listing of the prognostic, diagnostic and forcing variables is given in Table 1.

From the calculations outlined in Sections (3.1) through (3.4) equations (10) and (11) reduce to a pair of coupled differential equations in T_c and T_{gs} (see Section 4) which are solved by a numerical method.

3.1. Classification of the World's Biomes

The vegetation communities covering the earth's surface have been classified and identified on a 1° x 1° grid scale (Willmott et al., 1984) using data originating from Matthews (1983) and other sources. Currently, the classification identifies 32 surface cover types but, for the initial implementation of SiB, these categories are combined into 8 biomes. Each of these biomes has values for the surface properties listed in Table 2. In the non-interactive version of SiB, phenological variations in the surface properties are specified at one-month time resolution.

These basic data for each biome class give secondary parameters used by the SiB model (see following sections). This preliminary task, which need be done once only for each biome, is performed by the SiB preprocessor.

3.2. Radiation Balance

The interception and scattering of radiation by vegetation may be modeled in a variety of ways (see the review of Dickinson, 1983), but a simple, economical method is appropriate to SiB.

The two-stream approximation description as described in Meador and Weaver (1980), Coakley and Chylek (1975) and Dickinson (1983), allows for the multiple scattering of light by leaves. Equations (12) and (13) were

Vegetation (Upper story)

z_2 - height of canopy top, m

z_1 - height of canopy base, m

Ld - leaf area density as a function of time, $m^2\ m^{-3}$

α,δ - leaf optical properties (reflection and transmission).

$O(\phi,\xi)$ - leaf angle distribution.

C_d, p_s - drag coefficient of leaves, shelter factor

C_s - leaf transfer coefficient

a,b,c - stomatal resistance coefficients (light dependence).

T_l,T_h,T_o - minimum, maximum and optimum temperatures for stomatal functioning, K

h_5 - parameter governing stomatal response to vapor pressure, $mbar^{-1}$

h_6, ψ_c - parameters governing stomatal response to leaf water potential m^{-1}, m

S_c - precipitation interception capacity, m

V_c - extent of surface covered by upper story

C_c - heat capacity of vegetation, taken to be equivalent to 0.2 mm water per unit Leaf Area Index, $J\ m^{-2}\ K^{-1}$

z_d,D_d - rooting depth and density as functions of time, m, $m\ m^{-3}$

r_{plant} - resistance imposed by plant vascular system, s

R - root resistance per unit root length, $s\ m^{-1}$

Where there is significant ground cover underneath the upper story vegetation, parameters corresponding to the above list are also required for the lower storey except for z_2, z_1, L_d, C_c, C_d, p_s and C_s and with the addition of:

L_t - total leaf area index, $m^2\ m^{-2}$

z_s - roughness length of ground, m, or

C_{D_g} - drag coefficient of the ground

Soil

C_g - effective heat capacity of the ground, $J\ m^{-2}\ K^{-1}$ (see Section 4.4)

D_1 - depth of interception layer, m

D_2 - depth of upper story root zone, m

D_3 - depth of recharge zone, m

K_s - saturated conductivity, $m\ s^{-1}$

S_p - pore space

ψ_s - soil moisture potential at saturation, m

B - soil moisture potential parameter

α_s - soil optical properties

Table 2: Biome surface properties from which SiB parameters are derived (see Section 4.1).

proposed by Dickinson (1983) as appropriate for vegetation.

$$-\bar{\mu}\frac{dI\uparrow}{dL} + [1-(1-\beta)\omega]\, I\uparrow - \omega\beta I\downarrow = \omega\bar{\mu}K\beta_0 e^{-KL} \qquad (12)$$

$$\bar{\mu}\frac{\partial I\downarrow}{dL} + [1-(1-\beta)\omega]\, I\downarrow - \omega\beta I\uparrow = \omega\bar{\mu}K(1-\beta_0)e^{-KL} \qquad (13)$$

$I\uparrow, I\downarrow$ = upward and downward diffuse radiative fluxes, normalized by the incident flux

K = optical depth of the direct beam per unit leaf area

$= G(\mu)/\mu$

$G(\mu)$ = projected area of leaf elements in direction μ

μ = cosine of the zenith angle of the incident beam

$\bar{\mu}$ = average inverse diffuse optical depth per unit leaf area

$= \int_0^1 [\mu'/G(\mu')]\, d\mu'$

μ' = direction of scattered flux

ω = scattering coefficient

L = cumulative leaf area index

and β and β_0 are the upscatter parameters for the diffuse and direct beams, respectively. The value of $\omega\beta$ is inferred from the analysis of Norman and Jarvis (1975):

$$\omega\beta = 1/2\, [\alpha + \delta + (\alpha - \delta)\cos^2\bar{\theta}] \qquad (14)$$

$\omega = \alpha + \delta$

α = leaf reflection coefficient

δ = leaf transmission coefficient

$\bar{\theta}$ = mean leaf angle inclination above the horizontal plane

The value of β_0, the direct beam upscatter parameter, was suggested

by Dickinson (1983) to be:

$$\beta_o = \frac{(1 + \bar{\mu}K)}{\omega\bar{\mu}K} \cdot a_{s(\mu)} \qquad (15)$$

where the single scattering albedo, $a_{s(\mu)}$ is given by:

$$a_{s(\mu)} = \omega \int_0^1 \frac{\mu' \, \Gamma(\mu,\mu')}{[\mu \, G(\mu') + \mu' G(\mu)]} \, d\mu' \qquad (16)$$

$$\Gamma(\mu,\mu') = G(\mu) \, G(\mu') \, P(\mu,\mu')$$

$$P(\mu,\mu') = \text{scattering phase function}$$

A full discussion of the various terms in (12) to (16) is presented in the comprehensive review of Dickinson (1983).

A number of simplifying assumptions are made for calculating some of the above parameters for use within SiB, for example, all the individual scattering interactions are taken to be isotropic which makes the scattering phase function independent of the angle of the incoming beam. The physical implications of these assumptions and the method of obtaining solutions to (12) and (13) are discussed in Sellers (1985a). After some manipulation, (12) and (13) may be modified and solved with suitable boundary conditions for the albedo and transmission coefficient of the canopy (see Sellers, 1985a), for both direct beam and diffuse incident radiation. To take account of the effects of non-uniform plant cover, we let V_c and V_g represent the fractional cover of the upper story and ground vegetation respectively. The area averaged leaf area index, $\overline{L_t}$, is related to the local leaf area index, $\overline{L_t}$, used in the radiation calculation by $L_t = \overline{L_t}/V$ where $V = V_c$, V_g and $L_t = L_{tc}$, L_{tg}. The albedo of the ground (ground cover plus bare soil) is then given by

$$A_{\Lambda,\mu} = I\uparrow_g \cdot V_g + (1 - V_g)\,\alpha_{s(\Lambda)} \tag{17}$$

$A_{\Lambda,\mu}$ = ground albedo as a function of wavelength interval, Λ, and angle of incident radiation, μ

α_s = soil reflectance

$I\uparrow_g$ = upward diffuse radiation flux above ground cover, normalized by the incident flux

and $A_{\Lambda,\mu}$ for diffuse and direct fluxes is $A_{\Lambda,d}$ and $A_{\Lambda,b}$, respectively.

The radiation absorbed by the canopy and ground is then

$$F_{\Lambda,\mu(c)} = V_c(1-I\uparrow_c - I\downarrow_g^c\,(1-A_{\Lambda,d}) - e^{-KL_{tc}}\,(1-A_{\Lambda,b})) \cdot F_{\Lambda,\mu(0)} \tag{18}$$

and

$$F_{\Lambda,\mu\,(g)} = \{\,(1-V_c)(1-A_{\Lambda,\mu}) + V_c\,[I\downarrow_g^c\,(1-A_{\Lambda,d}) + e^{-KL_{tc}}\,(1-A_{\Lambda,b})]\,\} \times F_{\Lambda,\mu(0)} \tag{19}$$

$F_{\Lambda,\mu(0)}$ = incident radiant energy of wavelength interval Λ and direction μ, W m^{-2}

$F_{\Lambda,\mu(c)}$, $F_{\Lambda,\mu(g)}$ = amount of $F_{\Lambda,\mu(0)}$ absorbed by the canopy and by the ground cover and soil, W m^{-2}

$I\uparrow_c$ = diffuse flux leaving top of canopy

$I\downarrow_g^c$ = diffuse flux leaving base of canopy

$e^{-KL_{tc}}$ = direct flux penetrating the canopy

= 0, when μ = d

L_{tc} = local leaf area index of canopy, m^2 m^{-2}

d,b = subscripts for diffuse and direct beam components, respectively

(N.b.: The diffuse terms in (18) and (19) are normalized by the incident flux, $F_{\Lambda,\mu}(0)$. Also, $A_{\Lambda,b}$ will vary with solar angle while $A_{\Lambda,d}$ is constant for a given surface condition.)

The above calculations are done for five components of the incoming radiation: visible (diffuse and direct), near infrared (diffuse and direct) and thermal infrared (diffuse only). Mean values of the reflection and transmission coefficients for the leaves and soil are used within each wavelength interval.

Finally, the net radiation terms are calculated by subtracting the emitted thermal radiative loss from the absorbed radiative terms.

$$Rn_c = \langle F_c \rangle - 2\sigma_s T_c^4 . V_c + \sigma_s T_{gs}^4 . V_c \qquad (20)$$

$$Rn_{gs} = \langle F_{gs} \rangle - \sigma_s T_{gs}^4 + \sigma_s T_c^4 . V_c \qquad (21)$$

$\langle F_c \rangle$, $\langle F_{gs} \rangle$ = sum of the 5 absorbed radiation components, W m^{-2}

σ_s = Stefan-Boltzman constant, W m^{-2} K^{-4}

T_c, T_{gs} = canopy, ground temperatures, K

In (20) and (21), the emissivities of ground and canopy are assumed to be unity.

Figure 5 indicates the performance of the radiation model. The global hemispherical albedo observed over a spring wheat crop in West Germany is shown for two summer days in 1979 (van der Ploeg et al.; 1980). Also shown is the predicted albedo for a wheat cover at a similar growth stage at a nearby site as given by (12) and (13). The diurnal trend and magnitudes of the predicted global albedo agree broadly with the observations.

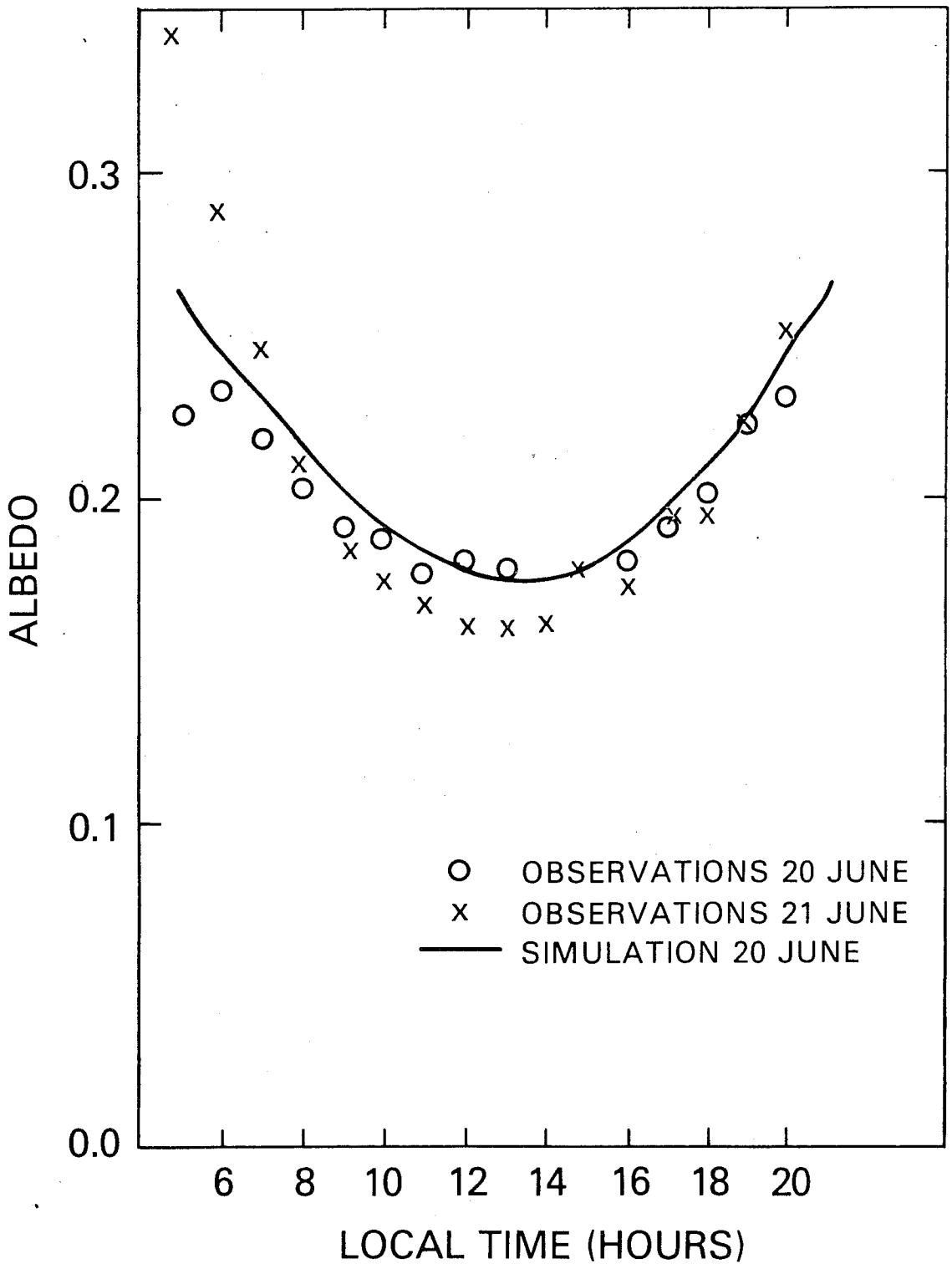

Fig.5 Measured and simulated albedo values for short wave radiation above a wheat crop. The observed points were calculated from observations of incoming and outgoing short wave radiation taken at Volkenrude, W.Germany, June 20-21, 1979, by van der Ploeg et al (1980). The simulation for the what crop at Ruthe (50 km away) for June 20, 1979 is also shown (see Section 3.2. in text).

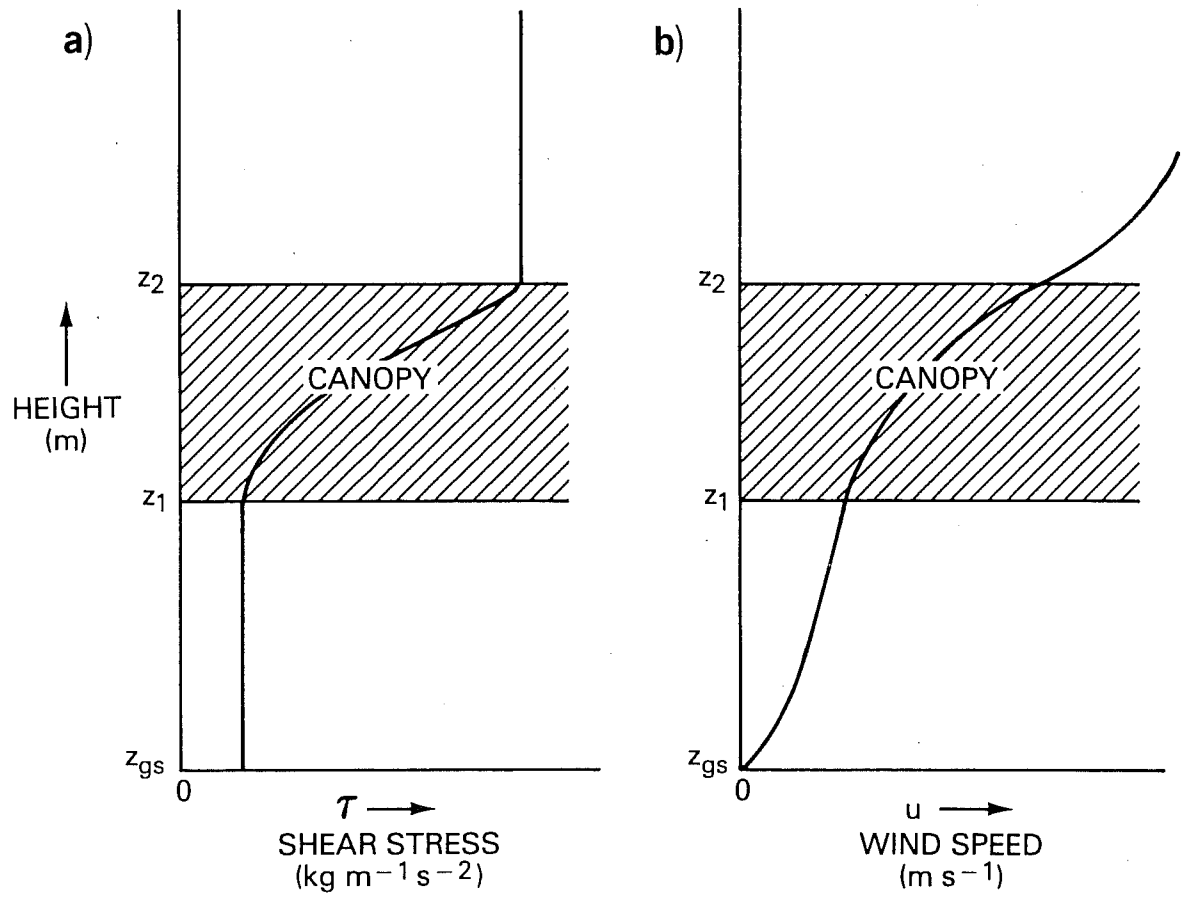

Fig.6 Profiles of (a) shear stress and (b) wind speed above, within and below the canopy as represented in SiB.

3.3. Aerodynamic Resistances

Figure 4 shows how the SiB model transfers heat and vapor from canopy and ground via three aerodynamic resistances and two surface resistances. The turbulent transport of momentum and other quantities between the atmosphere simply modeled (see Raupach and Thom, 1981). In SiB, flux-gradient descriptions describe all such transfers, although such methods are not completely realistic.

Some of the data listed in Table 2 are used to solve diffusion equations which describe the absorption of momentum by the surface. Figure 6 shows how the upper story canopy is represented as a block of constant-density porous material sandwiched between two constant-stress layers. Extrapolation of the log profile yields underestimates of the turbulent transfer coefficient close to the top of the canopy. Thus, the log profile is only valid above a certain transition height, z_m, which is taken to be a function of surface morphology. Below this level, an empirical adjustment to the profile must be made. Data from Garratt (1978) and Raupach and Thom (1981) are used to estimate the value of z_m as equal to $z_2 + 2\ (z_2 - d)$, and the ratio of the actual turbulent transfer coefficient at z_2 to that predicted by the log profile as ~ 2.0. Under neutral conditions, equations for the transfer of momentum above and within the canopy are:

Above the canopy: $z > z_m$

$$\tau = \rho\, u_*^2 = \rho \left(\frac{ku}{\ln \frac{z-d}{z_0}} \right)^2 \qquad (22)$$

τ = shear stress, kg $m^{-1}s^{-2}$

ρ = air density, kg m^{-3}

u_* = friction velocity, m s^{-1}

k = von Karman's constant = 0.41

d = zero plane displacement height, m

z_o = roughness length, m

z_m = transition height, m

Within the canopy: $z_1 < z < z_2$

$$\frac{\partial \tau}{\partial z} = \rho \frac{Cd\ \overline{Ld}}{\rho_s} \cdot u^2 \tag{23}$$

u = wind speed, m s^{-1}

Cd = leaf drag coefficient

$\overline{Ld}$ = area-averaged leaf area density, $m^2\ m^{-3}$

ρ_s = leaf shelter factor

Also:

$$\tau = \rho K_m \frac{\partial u}{\partial z} \tag{24}$$

K_m = momentum transfer coefficient $m^2\ s^{-1}$

and

$$d = \frac{\int_{z_1}^{z_2} u^2\, z\, dz}{\int_{z_1}^{z_2} u^2\, dz + \frac{\tau}{\rho}\Big|_{z_1} \frac{P_s}{\overline{Ld}\ Cd}} \tag{25}$$

and

$$K_m = \sigma \cdot u \tag{26}$$

σ = constant, m

Equations (22), (23) are commonly used to describe the absorption of momentum by a rough surface and are derived in Monteith (1973). Equation (25) was first suggested by Thom (1971) where d, the zero plane displacement height, is defined as the moment height for momentum absorption. The second term, $\tau/\rho|_{z1}$ $(p_s/Ld\ Cd)$, has been added to the original form to account for the momentum absorbed by the ground. In contrast to the approach used in describing radiative transfer, the effects of vegetation morphology on turbulent transfer are described in terms of the area-averaged (denoted by an overbar) properties of the plant cover.

In order to calculate the momentum transfer characteristics of the surface, z_o and d, and to estimate the values of the resistances $\overline{r_b}$, r_d and r_a, equations (22) to (25) are closed by adding another equation describing the variation of K_m within the canopy air space. Currently, the assumption that K_m is proportional to the local wind speed is used within the canopy; see (26). The equation set may then be solved to yield values of σ , z_o, d and hence profiles of u and K_m above, within and below the canopy. Boundary conditions are provided by the wind speed at reference height, u_r, and the shear stress at the ground, a function of wind speed at the canopy base, $u|_{z1}$, and the ground drag coefficient, C_{Dg}. Although the use of 'K-theory' within the canopy is physically unrealistic, it yields reasonable results, so this simple analysis is to be used until suitable second order closure models are applied to the problem.

The calculated profiles of u and K_m give the aerodynamic resistances; r_a, $\overline{r_b}$ and r_d. The explicit forms of r_a, $\overline{r_b}$ and r_d are not reproduced here but may be found in the Appendix of Sellers et al. (1985).

First, $\overline{r_b}$: The laminar boundary layer resistance for a single leaf has been determined experimentally for many species (Goudriaan; 1977) and commonly yields an expression of the form

$$r_{b_i} = \frac{C_s}{L_i \sqrt{u_i}} \tag{27}$$

C_s = transfer coefficient (dependent on leaf shape and size)

L_i = leaf area of i^{th} leaf, m^2

u_i = local wind speed, $m\ s^{-1}$

r_{b_i} = boundary layer resistance of i^{th} leaf, $s\ m^{-1}$

A bulk boundary layer resistance may be assigned to a group of leaves if the individual resistances, r_{b_i}, are assumed to act in parallel. As the variation of u with height within the canopy is known from the solution of (22) to (26), we may write

$$\frac{1}{\overline{r_b}} = \int_{z_1}^{z_2} \frac{\overline{Ld\sqrt{u(z)}}}{\rho_s C_s}\, dz \tag{28}$$

$\overline{r_b}$ = area-averaged bulk boundary layer resistance, $s\ m^{-1}$

For neutral conditions (28) gives

$$\overline{r_b} = \frac{C_1}{\sqrt{u_2}} \tag{29}$$

u_2 = wind speed at z_2

C_1 = surface dependent constant obtained by integrating (28).

The vapor and sensible heat source height, h_a, is taken as the center of action of $\overline{r_b}$ in the canopy such that $\int_{z_1}^{h_a} r_b^{-1} \cdot dz = \int_{h_a}^{z_2} r_b^{-1} \cdot dz$

The neutral value of the aerodynamic resistance r_d for the transfer of heat and water vapor between the soil surface and h_a is simply

$$r_d = \int_0^{h_a} \frac{1}{K_m} dz = \frac{C_2}{u_2} \tag{30}$$

C_2 = surface/canopy dependent constant

The aerodynamic resistance between h_a and z_r is r_a, defined as

$$r_a = \int_{h_a}^{z_r} \frac{1}{K_s} dz = \int_{h_a}^{z_2} \frac{1}{K_{s(z)}} dz + \int_{z_2}^{z_r} \frac{1}{K_{s(z)}} dz \tag{31}$$

K_s = heat and vapor transfer coefficient, $m^2\ s^{-1}$

Under neutral conditions,

$$r_a = \frac{C_3}{u_r} \tag{32}$$

C_3 = surface dependent constant

u_r = wind speed at reference height, ms^{-1}

The above expressions for $\overline{r_b}$, r_d and r_a are modified to account for the effects of non-neutrality and, in the case of $\overline{r_b}$ and r_d, u_2 is replaced by u_r. The relationship between u_2 and u_r and the full forms of the non-neutral resistances are given in the Appendix of Sellers et al. (1985).

The coefficients C_1, C_2, z_o and d are calculated only once for a given surface configuration by a preprocessor program. The non-neutral calculation of r_a depends on z_o, d and the Monin-Obukhov length; (32) is only valid under neutral conditions.

The sensitivity of the derived parameters z_o, d, r_a, $\overline{r_b}$ and r_d to errors in the estimates of the input variables has been explored. Figures 7 show

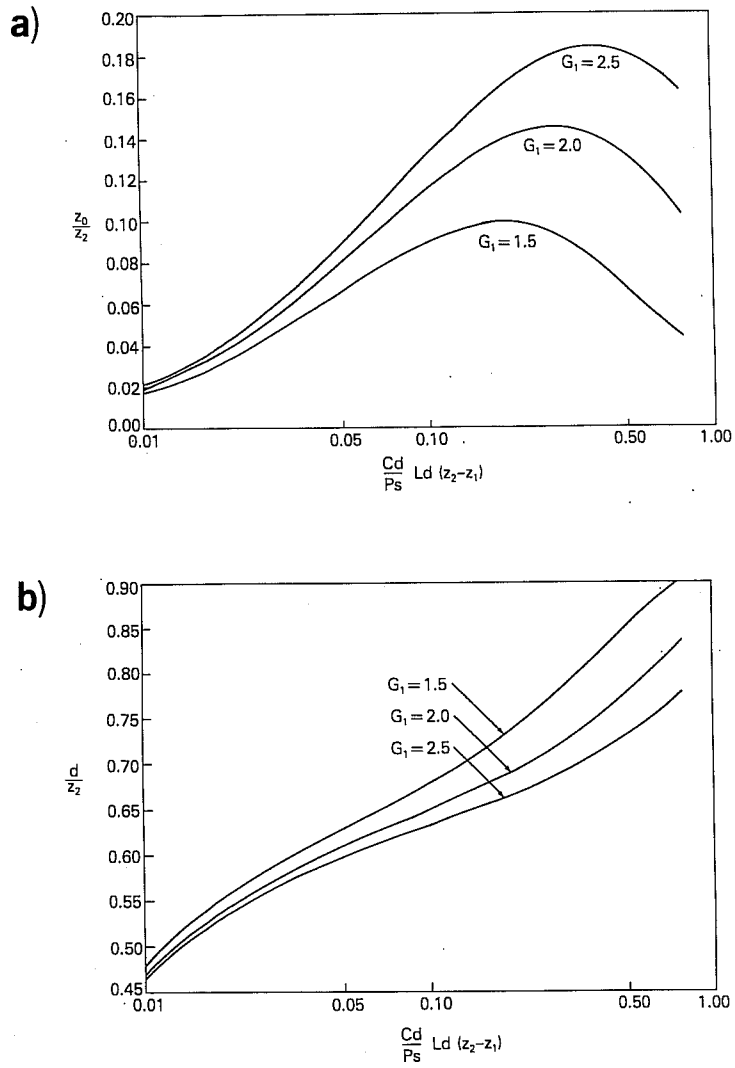

Fig.7 (a) Roughness length, z_o and (b) zero plane displacement height, d, both normalized by canopy height z_2 and versus a non-dimensional parameter given by the product of the drag coefficient, leaf area index and shelter factor, which is equivalent to the total drag coefficient of the canopy as used by Shaw and Pereira (1982), Figs.4 and 5. The variation of z_o and d is shown for various values of the parameter G_1. G_1 is the ratio of the actual value of K_m at z_2 to the estimate provided by an extrapolation of the log-linear wind profile.

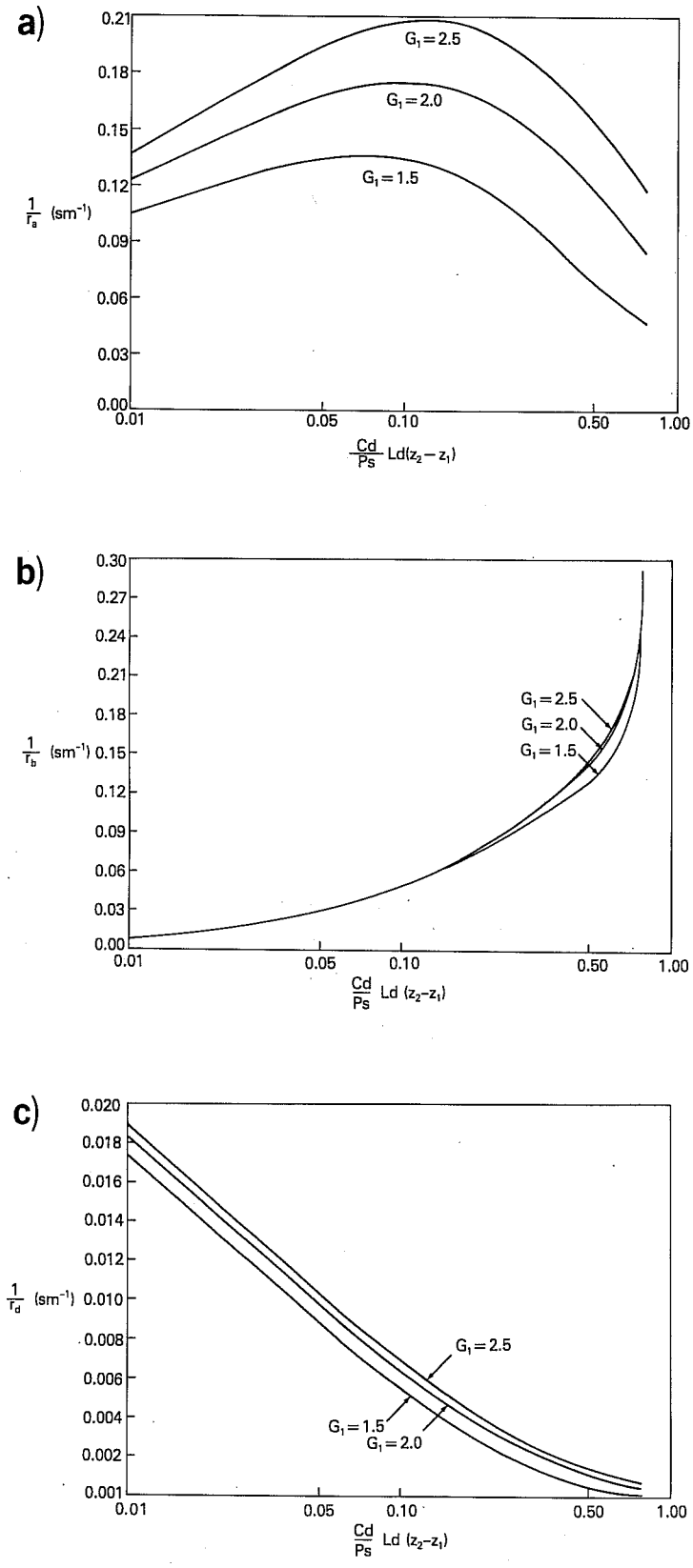

Fig.8 Variation of the inverse of the aerodynamic resistances (a); r_a, (b); $\bar{r}_b$ and (c), r_d with increasing canopy drag coefficient for a range of G_1 values (see text and caption for Fig.8). Simulations are for a wind speed of 10 m s^{-1} at 15 m, z_2 = 5 m, z_1 = 1 m and neutral conditions.

the predicted variation in z_0 and d with increasing total canopy drag coefficient; Cd $\overline{Ld}$ $(z_2 - z_1)/p_s$. The results compare well with those of Shaw and Pereira (1982) which were obtained with a second order closure model and also with measured values found in the literature. It is clear that large errors in the total leaf area index $\overline{Ld}$ $(z_1 - z_2)$, the effective leaf element drag coefficient Cd/p_s and the ratios of the actual value of K_m at z_2 and the aerodynamic resistance between z_2 and z_m, G_1 and G_2 respectively, can have moderate effects on the predicted values of z_0 and d. (The values of $G_1 = 2.0$ and $G_2 = 0.5$ currently used in the model are taken from the results published in Raupach and Thom; (1981): these seem to produce results most consistent with those of Shaw and Pereira (1982)). However, as figure 8 shows, such errors have a reduced effect on the magnitudes of r_a, $\overline{r_b}$ and r_d; mainly as these quantities are dependent upon the inverse logarithm of z_0. Furthermore, additional sensitivity studies have shown (Sellers and Dorman; in prep.) that while the partition of energy at the surface is sensitive to the magnitudes of the aerodynamic resistances, changing them by up to a factor of 2 or more had relatively little effect on the daily totals of sensible and latent heat released by the surface.

3.4. Surface Resistances and Vapor Fluxes

3.4.1. Transpiration and Evaporation from the Soil Surface

The resistances to the transport of moisture from a theoretically saturated air space at the temperature of the canopy or from the ground to the free air are defined as the canopy resistance, $\overline{r_{st}}$, ground vegetation resistance, r_g, and soil surface resistance, r_{surf}, respectively. When the canopy is dry, $\overline{r_{st}}$ is assumed to be equivalent to the resistances of all the leaf stomata acting in parallel. Similarly, the resistance to vapor transfer at the ground level is a combination of the bulk stomatal

resistance of the ground vegetation, r_g, and the diffusion resistance of the soil surface, r_{surf}.

Jarvis (1976) summarized his own and other researcher's work on the stomatal function of coniferous trees. The stomatal resistance of an individual leaf, r_s, was taken to be a function of the incident visible radiative flux, $F_{s,\downarrow}$, vapor pressure deficit (T_a, e_a), leaf temperature, T, and leaf water potential, ψ_ℓ. Rearrangement of Jarvis' original expression yields

$$r_s = \frac{a}{b + F_{s\downarrow}} + c \cdot f(\psi_\ell)^{-1} \cdot f(T)^{-1} \cdot f(T_a,e_a)^{-1} \qquad (33)$$

a,b,c = constants determined from observations

$F_{s,\downarrow}$ = short wave flux incident on leaf surface, W m^{-2} (0.4 - 0.7 μm wavelength interval)

$f(\psi_\ell), f(T), f(T_a,e_a)$ = factors limiting stomatal resistance depending on leaf water potential ψ_ℓ, leaf temperature, T, and air vapor pressure deficit, $e*(T_a)-e_a$. All factors are limited to $0 \leq f(\ ) \leq 1$

= $f(\Sigma)$

Following a methodology similar to that used for the derivation of r_b in (26), we define the <u>bulk</u> stomatal resistance for the canopy by:

$$\frac{1}{\overline{r_{st}}} = \int_0^{\overline{L_t}} \int_0^{\pi/2} \int_0^{2\pi} \frac{O(\xi,\theta)}{r_s} \text{Sin } \theta \, d\xi \cdot d\theta \cdot dL \qquad (34)$$

$O(\xi,\theta)$ = leaf angle distribution function

ξ,θ = leaf azimuth, inclination angles

The extinction of short wave or photosynthetically active radiation (PAR) down through the canopy has been described by (12) and (13). In view of the small amount of scattering by leaves in this wavelength interval, ($\omega \leq 0.2$), the extinction of PAR is approximated by Goudriaan's (1977) semi-empirical expression to yield a more manipulable function:

$$F_{s(L)} \simeq F_{s(0)} \exp(-\kappa \cdot L) \tag{35}$$

κ = extinction coefficient

$$= \frac{G(\mu)}{\mu} (1-\omega_s)^{1/2}$$

$F_{s(0)}$ = shortwave flux above canopy, W m^{-2}

$F_{s(L)}$ = shortwave flux within canopy below a leaf area index of L, W m^{-2}

ω_s = leaf scattering coefficient for PAR

With an appropriate value of $G(\mu)$ used in (35), and with the assumption that leaf water potential, air temperature and humidity vary only slightly within the canopy when compared to the extinction of radiation, (34) is simplified to

$$\frac{1}{\overline{r_{st}}} \simeq V_c \cdot N_c \cdot f(\Sigma) \int_0^{L_{tc}} \int_0^{\pi/2} \int_0^{2\pi} \frac{O(\xi,\theta)}{r_s(F_{s,\mu(o)}, \kappa, \xi, \theta)} \sin\theta \, d\xi \cdot d\theta \cdot dL \tag{36}$$

$f(\Sigma) = f(\psi_\ell) \cdot f(T) \cdot f(T_a, e_a)$

N_c = fraction of L_{tc} made up of live, photosynthesizing leaves

Some analytical solutions to the integral part of the above equation for a number of leaf angle distribution functions are discussed by Sellers

(1985)a. The dependences on leaf water potential, vapor pressure deficit and leaf temperature are currently the same as in Jarvis (1976), whereby optimum conditions result in setting the respective factor to 1 and less than optimal conditions reduce it, thus increasing the total resistance.

The factor $f(\psi_\ell)$ accounts for the effects of soil moisture stress and excessive evaporative demand.

$$f(\psi_\ell) = 1 - \exp(-h_6 \delta\psi) \tag{37}$$

$$\delta_\psi = \psi_\ell - \psi_o$$

ψ_o = leaf water potential at which stomata close completely, m

h_6 = species dependent constant, m^{-1}

The quantity ψ_ℓ is calculated with a catenary model of the water transfer pathway from root zone to leaf given by van der Honert (1948):

$$\psi_\ell = \psi_r - z_T - \frac{E_d}{\rho_w} (\overline{r_{plant}} + \overline{r_{soil}}) \tag{38}$$

ψ_ℓ = leaf water potential, m

z_T = height of transpiration source, m

= h_a for upper story vegetation

= 0 for ground vegetation

ψ_r = soil moisture potential in root zone, m

$\overline{r_{plant}}$ = area-averaged resistance imposed by plant vascular system, s

$\overline{r_{soil}}$ = area-averaged resistance of soil and root system, s

ρ_w = density of water, kg m^{-3}

E_d = transpiration rate, kg m^{-2} s^{-1}

The soil moisture potential in the root zone, ψ_r, is an average term obtained by summing the weighted soil moisture potentials of the soil layers from the surface to the rooting depth, z_d.

$$\psi_r = \sum_{o}^{z_d} \frac{\psi_i D_i}{z_d} \tag{39}$$

ψ_i = soil moisture potential of the ith layer, m

D_i = depth of the ith layer, m

z_d = rooting depth, m

The soil moisture potential of a layer, ψ_i, is given by the empirical expression of Clapp and Hornberger (1978):

$$\psi_i = \psi_s W_i^{-B} \tag{40}$$

W_i = soil moisture wetness fraction

ψ_s = soil moisture potential at saturation, m

B = empirical constant

The area-averaged resistance imposed on the flow of water from the soil to the root cortex, $\overline{r_{soil}}$, is described by a depth-averaged form of the expression proposed by Federer (1979).

$$\overline{r_{soil}} = (R/D_d + \alpha_f/K_r)/z_d$$

$$\alpha_f = \frac{1}{8\pi D_d} \left[\left(V_r - 3 - 2 \ln \left(\frac{V_r}{1-V_r}\right)\right)\right] \tag{41}$$

R = resistance per unit root length, s m^{-1}

D_d = root density, m m^{-3}

V_r = volume of root per unit volume of soil, m^3 m^{-3}

K_r = mean soil hydraulic conductivity in the root zone, m s^{-1}

The soil hydraulic conductivity in the root zone, K_r, is obtained by a manipulation of the expressions of Clapp and Hornberger (1978) and Milly and Eagleson (1982) which yields K_r as a function of ψ_r.

$$K_r = K_s(\psi_s/\psi_r)^{(2B+3)/B} \tag{42}$$

K_s = soil saturated hydraulic conductivity, m s^{-1}

Values of B, ψ_s and K_s for a number of different soils are listed in Clapp and Hornberger (1978). The transpiration rates from the dry portions of the vegetation are given by

$$\lambda E_{dc} = \frac{(e*(T_c) - e_a)}{\overline{r_{st}} + \overline{r_b}} \frac{\rho c_p}{\gamma} (1 - W_c) \tag{43}$$

$$\lambda E_{dg} = \frac{(e*(T_{gs}) - e_a)}{r_g + r_d} \frac{\rho c_p}{\gamma} (1 - W_g)\, V_g \tag{44}$$

E_{dc}, E_{dg} = transpiration rates of upper story, ground vegetation, kg m^{-2} s^{-1}

$e*(T_c)$, $e*(T_{gs})$ = saturated vapor pressure at temperatures, T_c, T_g, mbar

ρ, c_p = density, specific heat of air, kg m^{-3}, J kg^{-1} K^{-1}

γ = psychrometric constant, mbar K^{-1}

λ = latent heat of vaporization, J kg^{-1}

W_c, W_g = wetness fraction of upper story, ground vegetation

Following the calculation of the transpiration rates, the abstraction of water from the different soil layers is given by

$$E_{d_i} = \frac{D_i}{z_d} \left(\frac{\psi_i - \psi_\ell}{\overline{r_{plant}} + \overline{r_{soil}}}\right) \rho_w \tag{45}$$

E_{d_i} = extraction rate of transpired water from ith soil layer, kg m^{-2} s^{-1}

Equation (45) must be applied with values of E_d, ψ_ℓ and $\overline{r_{soil}}$ appropriate to the upper story and ground vegetation in turn. In the case of the ground vegetation, the rooting depth may not extend down to the bottom of D_2; ψ_r and E_{d_i} are then calculated using (39) and (45) except that the D_i terms are multiplied by the fractional depth of the soil layer which is occupied by the roots. All of the above calculations which relate stomatal resistance to the abstraction of soil water are performed for both the upper story and the ground vegetation.

There are few available data with which to test the efficacy of the above description of the plant water transfer system; in particular, the expression for bulk stomatal resistance. Monteith et al. (1965) measured the stomatal resistance of barley leaves with a viscous flow porometer and estimated the surface resistance of the crop as a residual of an energy balance calculation. Figure 9 shows their estimate of the surface resistance and the calculated value of $\overline{r_{st}}$ as provided by equation (36) assuming a spherical leaf angle distribution. The values of a, b and c were fitted onto the porometer data (see the upper points and solid line in Figure 9). The model appears to reproduce the trend in surface resistance reasonably well and also illustrates the diminishing effect of adding further increments of leaf area index -- the predicted difference in $\overline{r_{st}}$ for leaf area indices of 4 and 8 is relatively small as the additional leaves are shaded and hence have correspondingly high values of r_s.

Evaporation from the soil surface depends on the difference between the vapor pressure in the surface soil store W_1 and that of the canopy air

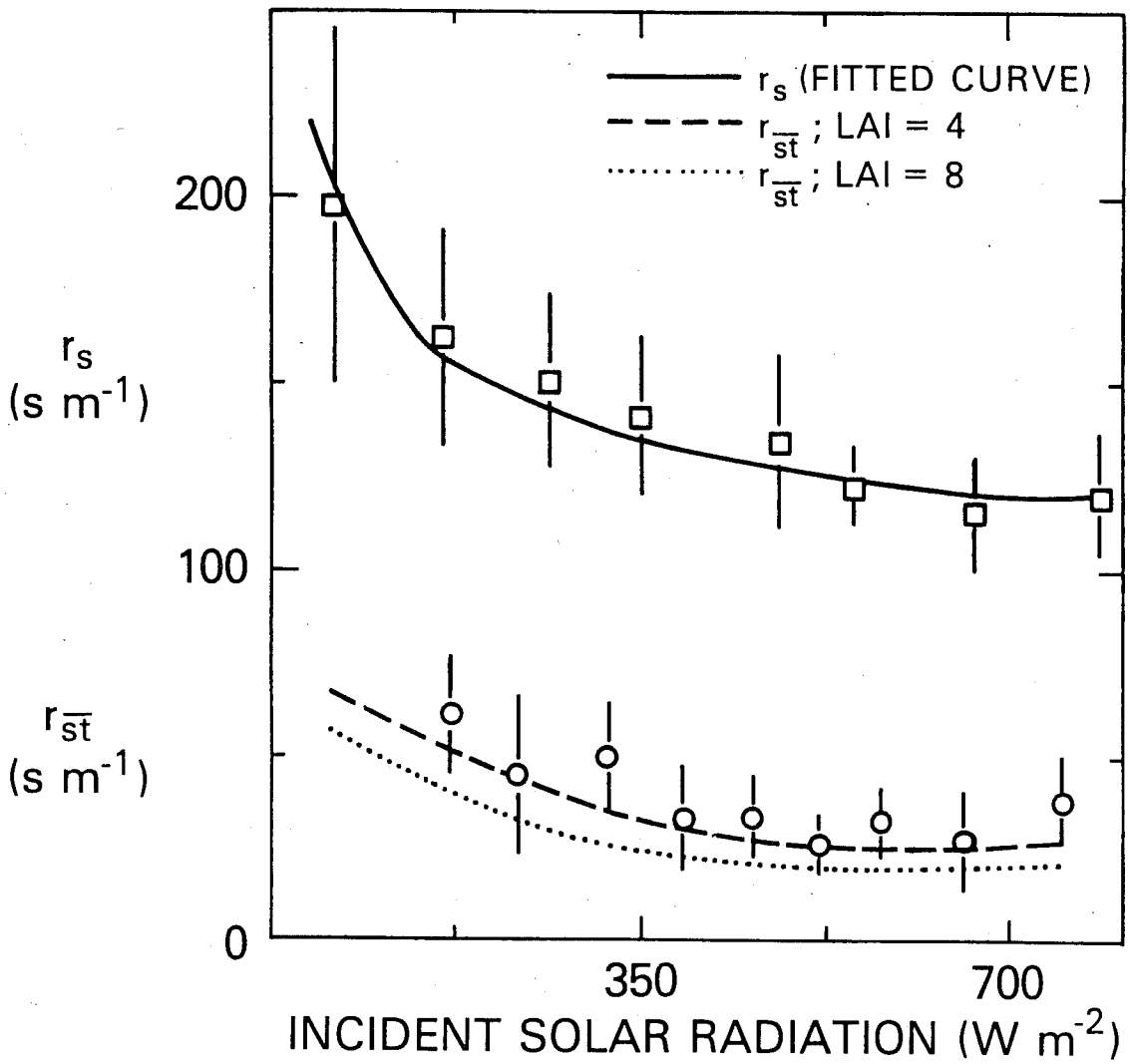

Fig.9 Data showing variation of leaf stomatal resistance, r_s, (top leaves) and anopy resistance, $\overline{r}_{st}$, for a barley crop (from Monteith et al., 1965). Lines show fit to r_s, using Eq. (33), and estimate of $\overline{r}_{st}$ as given by Eq. (34) in text for leaf area indices of 4.0 and 8.0.

space, e_a. Since the gradient of vapor pressure in the soil changes sharply near the surface, an empirical surface resistance term, r_{surf}, is used to account for the difference between the actual surface vapor pressure and the value associated with W_1 which is a mean value for the top few centimeters of soil (see Shu Fen Sun; 1982). Camillo and Gurney (1985) demonstrated that the specification of such an apparent soil surface resistance improved the performance of their multilayer soil model.

The evaporation rate from the soil is then expressed by

$$\lambda E_s = \frac{f_h \cdot e*(T_{gs}) - e_a}{r_d + r_{surf}} \frac{\rho c_p}{\gamma} \cdot (1 - V_g) \qquad (46)$$

E_s = soil evaporation rate, kg m^{-2} s^{-1}

f_h = relative humidity of water vapor in the surface soil moisture store

$= \exp(\psi_1 g/RT_g)$

ψ_1 = soil moisture potential of surface soil moisture store from (40), m

g = acceleration due to gravity, m s^{-2}

R = gas constant for water vapor, J kg K^{-1}

3.4.2 Interception and Interception Loss

The interception and evaporation of precipitation held on the leaf surfaces is modeled simply in SiB. The interception of rainfall is treated as equivalent to the interception of vertically incident radiation by black leaves. The inflow (interception) and outflow (drainage) of water stored on the canopy are then given by

$$P_c = P\,(1 - e^{-K_c L_{tc}})\,V_c \qquad (47)$$

$$D_c = 0,\ M_c < S_c$$

$$D_c = P_c,\ M_c = S_c$$

P = rainfall rate, m s^{-1}

P_c = rainfall interception rate of canopy, m s^{-1}

D_c = canopy drainage rate, m s^{-1}

M_c = water held on the canopy, m

S_c = maximum value of M_c, m
$\simeq$ (0.0002 to 0.0005) L_{tc}

K_c = extinction coefficient for canopy for black leaves and a vertical flux

= $G(\mu)/\mu$ where $\mu = 1$

For the ground vegetation:

$$P_g = (P - P_c + D_c)(1 - e^{-K_g L_{tg}})\,V_g \qquad (48)$$

$$D_g = 0,\ M_g < S_g$$

$$D_g = P_g,\ M_g = S_g$$

P_g = rainfall interception rate of ground vegetation, m s^{-1}

D_g = drainage rate of ground vegetation, m s^{-1}

M_g = water held on ground vegetation, m

S_g = maximum value of M_g, m

K_g = as for K_c but for ground vegetation

The input of precipitation into the soil surface moisture store is then given by

$$P_w = P - P_c - P_g + D_c + D_g \qquad (49)$$

P_w = rainfall interception of soil surface moisture store, m s^{-1}

The transfers described by equations (47) to (49) are performed at the beginning of the time step so that the vegetation water storage values, M_c and M_g, are determined prior to the energy balance calculations for the time step. The quantities M_c and M_g determine the fractional wetted areas of the canopy, W_c, and ground cover, W_g. Wetted areas have a surface resistance of zero. The evaporation rates from the wetted parts of the vegetation are given by

$$\lambda E_{wc} = \frac{(e*(T_c) - e_a)}{\overline{r_b}} \frac{\rho c_p}{\gamma} W_c$$

$$W_c = M_c/S_c, \; 0 \leq W_c \leq 1 \tag{50}$$

$$\lambda E_{wg} = \frac{(e*(T_{gs}) - e_a)}{r_d} \frac{\rho c_p}{\gamma} W_g V_g$$

$$W_g = M_g/S_g, \; 0 \leq W_g \leq 1 \tag{51}$$

E_{wc}, E_{wg} = evaporation rates from wet parts of the upper storey, ground vegetation, kg m^{-2} s^{-1}

The wet and dry parts of the canopy in (50) and (51) are assumed to be at the same temperature. A number of arguments and some evidence (see Hancock et al.; 1983) indicate that this assumption is more reasonable than assuming separate temperatures. The interception loss terms are implicit in the energy balance equations in Section 4 where they are combined with transpiration and soil evaporation terms to yield the total latent heat fluxes from canopy and ground.

The simplified approach outlined above is thought to provide acceptable estimates of interception loss rates and is considerably less complex than combined approaches (see Sellers and Lockwood, 1981) where interception,

drainage and evaporation are described simultaneously. Provided the time step of simulation is short (one hour or less), the two methods should not produce widely differing predictions.

3.5. Soil Model

A three-layer isothermal model is used to describe the vertical transfer of water in the soil. Transfer of water from one layer to another is calculated as by Milly and Eagleson (1982), and the soil heat capacity is represented by a diurnal skin depth (C_g, the heat capacity of the soil slab, is thermally equivalent to about 25 mm to 40 mm of water, depending on soil wetness) as outlined in Arakawa (1972). The drainage rate out of the bottom layer is controlled by the soil hydraulic conductivity and gravity.

These interlayer exchanges are calculated at the end of the time step since these processes are comparatively slow compared to the interception and partition of radiation. The extraction of transpired water from the root zones is also performed at this time.

4. DYNAMIC EQUATION SET FOR SiB

The framework of SiB as outlined in Figure 4 has been used to write down the dynamic equations describing T_c and T_{gs} as functions of time (see equations (10) and (11)). Assuming no storage of heat or moisture at any of the junctions of the resistance network, we write the area-averaged fluxes from soil and vegetation as follows:

From canopy air space to reference height.

Sensible heat.

$$H_c + H_{gs} = \frac{(T_a - T_r)}{r_a} \cdot \rho\, c_p \qquad (52)$$

T_a, T_r = air temperature at canopy source height and reference height respectively, K

H_c, H_{gs} = sensible heat flux from canopy, soil respectively, W m^{-2}

ρ, c_p = density, specific heat of air respectively, kg m^{-3}, J kg^{-1} K^{-1}

Latent heat.

$$\lambda E_c + \lambda E_{gs} = \frac{(e_a - e_r)}{r_a} \cdot \frac{\rho\, c_p}{\gamma} \qquad (53)$$

e_a, e_r = vapor pressure at canopy source height and reference height respectively, mbars

λE_c, λE_{gs} = latent heat flux from canopy, soil respectively, W m^{-2}

γ = psychrometric constant, mbar K^{-1}

Canopy to canopy air space.

$$H_c = \frac{2(T_c - T_a)}{\overline{r_b}} \cdot \rho\, c_p \qquad (54)$$

$$\lambda E_c = (e^*(T_c) - e_a) \cdot \frac{\rho\, c_p}{\gamma} \left(\frac{W_c}{\overline{r_b}} + \frac{1 - W_c}{\overline{r_b} + \overline{r_{st}}} \right) \qquad (55)$$

$e_*(T_c)$ = saturated vapor pressure at T_c, mbar

r_a = aerodynamic resistance between canopy source height and reference height, s m^{-1}

$\overline{r_b}$ = bulk leaf boundary resistance, s m^{-1}

$\overline{r_{st}}$ = bulk stomatal resistance, s m^{-1}

W_c = wetted fraction of canopy

Soil to canopy air space.

$$H_{gs} = \frac{(T_{gs} - T_a)}{r_d} \cdot \rho\, c_p \tag{56}$$

$$\lambda E_{gs} = (e^*(T_{gs}) - e_a) \frac{\rho\, c_p}{\gamma} \left[V_g \frac{W_g}{r_d} + \frac{1-W_g}{r_d + r_g} + \frac{(1-V_g)\, h_s}{r_{surf} + r_d} \right] \tag{57}$$

W_g = ground vegetation wetness fraction

r_g = surface resistance of ground vegetation (calculated in a similar way as $\overline{r_{st}}$), s m^{-1}

$e^*(T_g)_s$ = saturated vapor pressure at T_{gs}, mbar

h_s = factor to correct for soil dryness

$$= \frac{e^*(T_{gs})\, f_h - e_a}{e^*(T_{gs}) - e_a}$$

f_h = $\exp(\psi_1 g / R T_{gs})$

R = gas constant for water vapor, J kg^{-1} K^{-1}.

ψ_1 = soil moisture potential in top layer, m

In (55), stomata are assumed to be present on one side of the leaf only. Sensible heat is transfered from both sides of the leaf, hence the factor 2 in combination with the inverse of $\overline{r_b}$ in (54).

The preceding sections showed how the five resistances r_a, $\overline{r_b}$, r_d, $\overline{r_{st}}$ and r_g could be estimated. Given these values and the estimates of Rn_c and Rn_{gs} from section (3.1), equations (10) and (11) may be combined with

the above expressions to eliminate T_a and e_a and yield two equations in T_c and T_{gs} which may then be solved by an implicit backwards method (see Sellers et al., 1985).

Solution for the temperatures, and application of (53), (55), (57) over a time step will yield values of the latent heat fluxes λE_{wc}, λE_{wg} (interception losses), λE_{dc}, λE_{dg} (transpiration losses) and λE_s (soil surface loss). These fluxes are included in the calculation of the change of the five moisture stores.

A backwards implicit method was chosen for the solution of (52) through (57) because of its stability; however, it has been found that under changing radiative conditions and using time steps of more than half an hour, the solutions of T_c and T_{gs} show slight oscillation if no iterative corrections are made for the effects of non-neutrality on r_a.

A thorough evaluation of the performance of the various subcomponents of the model and their functioning as a separate ensemble is essential before implementing SiB in a GCM where unanticipated feedbacks between the boundary layer and surface models might obscure serious errors in the formulation.

Unfortunately, there are few complete sets of experimental data where input parameters, time series of forcing variables (u_r, T_r, e_r and the downward radiative fluxes) and time series of the generated fluxes and temperatures are all recorded. Two data sets which are almost complete in the above respects were used for the early, local, evaluations of the entire SiB model. The first consisted of biophysical and micrometeorological

measurements recorded for three days in June 1979 over a barley field in West Germany at part of a remote sensing experiment (see van der Ploeg et al. (1980) and Gurney and Camillo (1984)). Accordingly, the model parameters were fixed to represent a barley crop for which the necessary data sets were available. The morphological and physiological properties of the vegetation and the physical properties of the vegetation and soil were measured or estimated for the experimental site and were used to derive the model's surface parameters.

Since in this first case, the measurements were associated with a uniform, monoculture vegetation, it was not possible to perform a test of SiB in its full form as specified in this text; that is, with an upper story canopy and underlying ground vegetation. Hence we 'promoted' the crop canopy to the status of upper story vegetation and took the ground surface as bare so that $V_g = 0$. Initial soil moisture conditions were taken from van der Ploeg et al. (1980) and the micrometeorological data were then applied as the boundary forcing to the model in order to generate time series of the radiation exchanges, heat fluxes and surface temperatures.

Figure 10 compares the simulated course of $\overline{r_{st}}$ for the barley crop and some estimated bulk stomatal resistance values derived from individual leaf stomatal resistance observations. The predicted rise in $\overline{r_{st}}$ away from its light-limited value in the afternoon, because of the falling leaf water potential and decrease in $f(\psi_\ell)$, is in accordance with the trend of the observations.

Figure 11 shows the observed and predicted partitioning of the surface energy balance for the barley field. (The simulated net radiation was

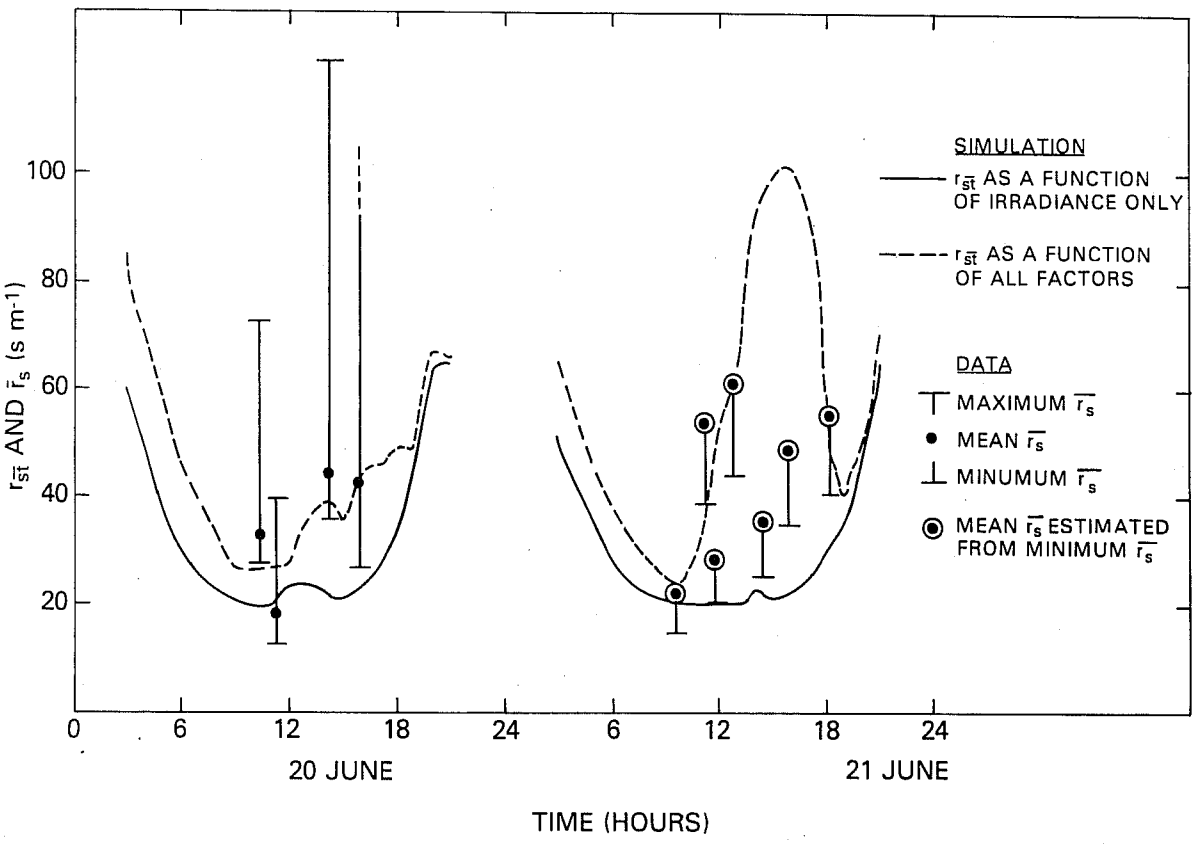

Fig. 10 Predicted (r_{st}) and estimated (r_s) values of the bulk stomatal resistance for the barley crop near Ruthe, W. Germany, June 20-21, 1979. Values of $\bar{r}_s$ were derived by summing the area-weighted conductances measured for upper, middle and lower leaves and then inverting the total. (A diffusion porometer was used to obtain the conductance values). Minimum r_s corresponds to the value of $\bar{r}_s$ for the topmost leaves weighted by the total leaf area index; maximum $\bar{r}_s$ is calculated in the same way except that r_s values for leaves at the canopy base were used.

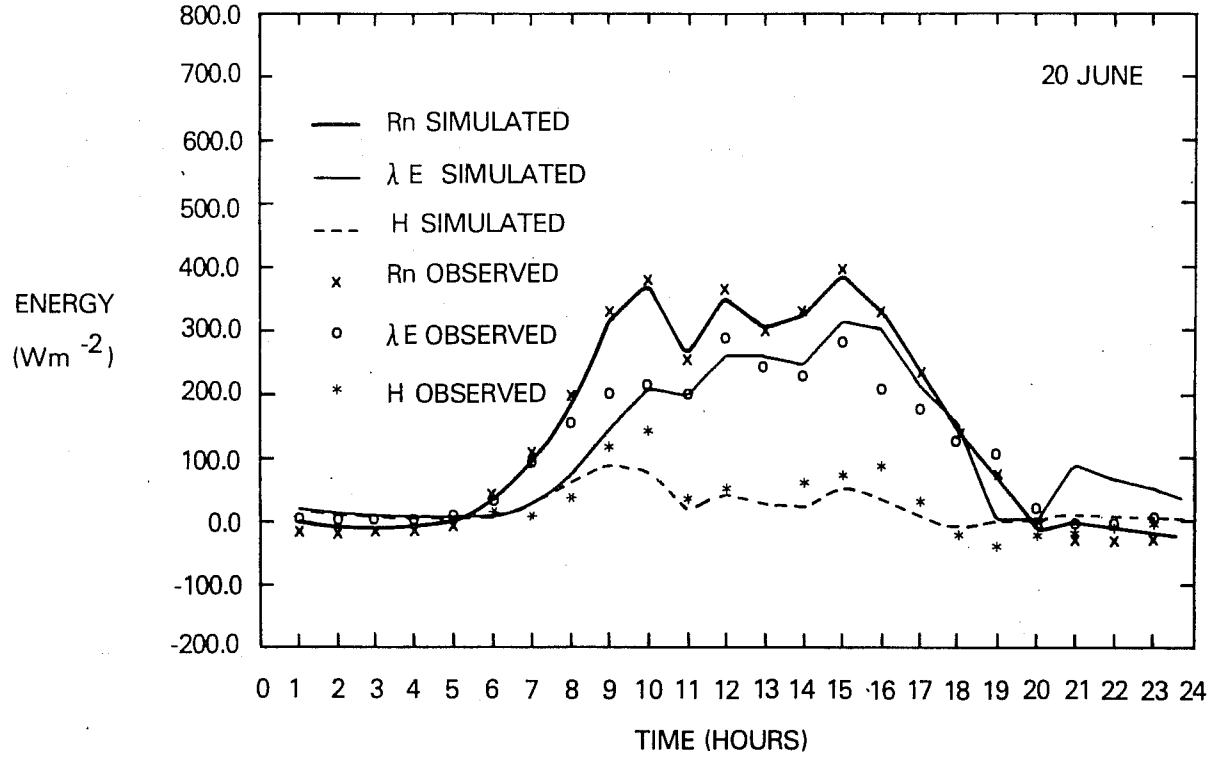

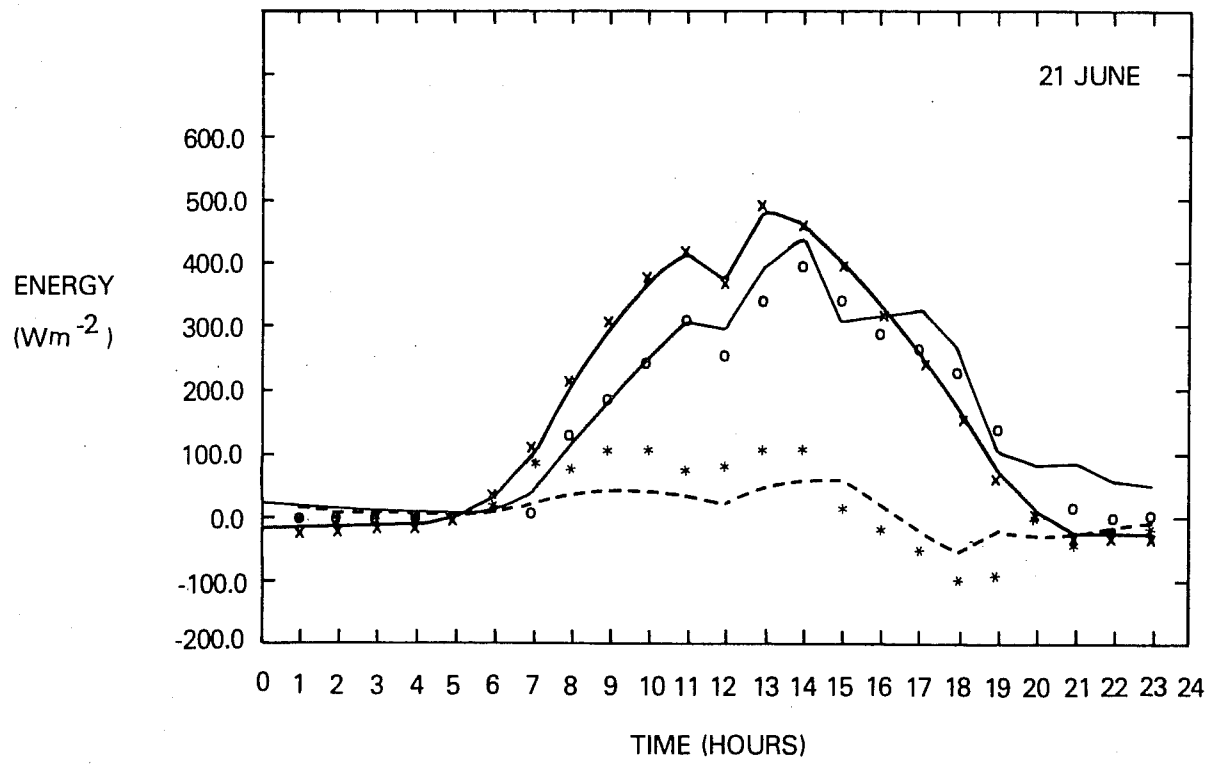

Fig. 11 Observed and predicted values of net radiation, R_n, latent heat flux, λE, and sensible heat flux, H for the barley test site, Ruthe, W.Germany for June 20-21, 1979. (The net radiation has been forced onto the observed values).

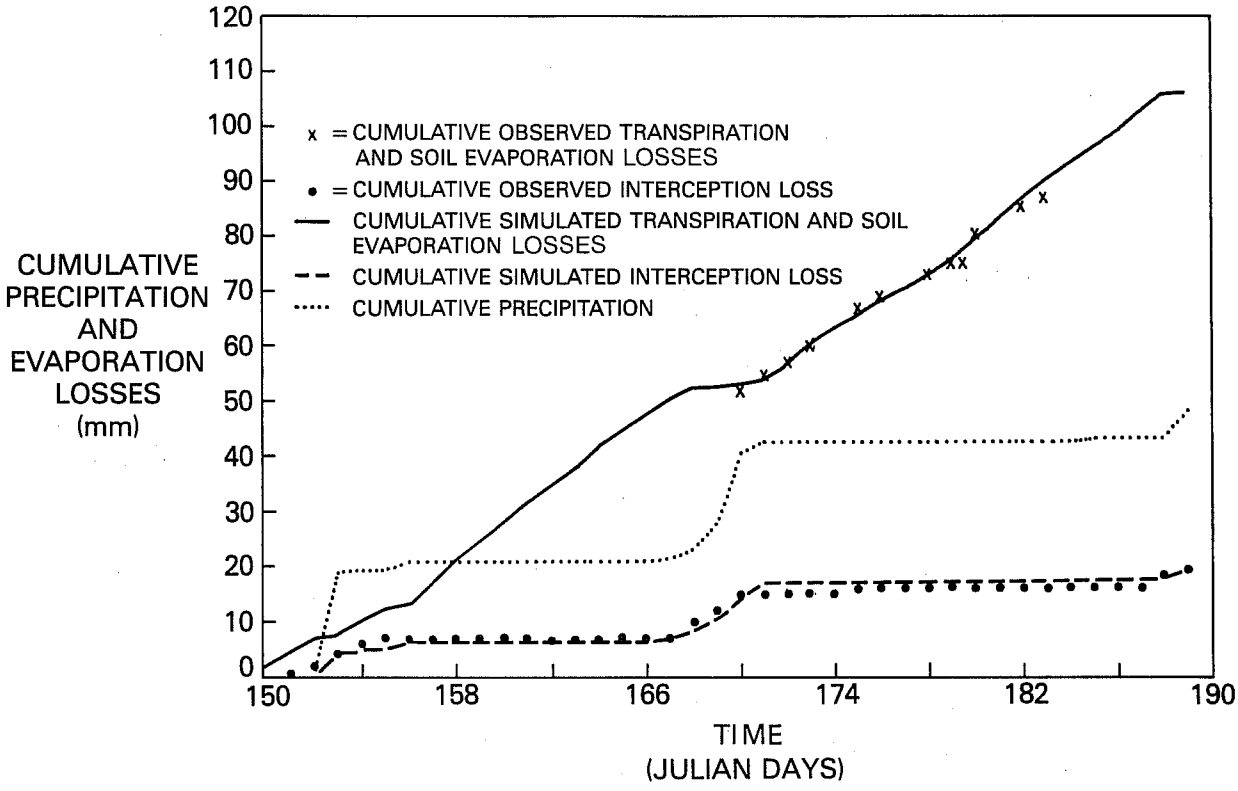

Fig. 12 Comparison of simulated (lines) and observed (dots) cumulative components of the water balance for the Plynlinon, Wales, U.K. forested lysimeter of Calder (1977). Cumulative precipitation is also shown for comparison with the interception loss simulations.

forced onto the observations as the long wave radiation flux measurements were severely in error.) The diurnal course and magnitudes of the predicted fluxes agree with the measurements.

The second data set consists of a time series of micrometeorological and radiative measurements recorded over a Sitka Spruce forest in Wales, United Kingdom during several months in 1975. Additionally, the water balance (precipitation, interception loss, transpiration and runoff) was monitored by means of an ingenious lysimetric technique (see Calder; 1977). Most of the input parameters for the model were provided by Calder and Roberts (pers. comm.), and the rest being taken from the ecological literature; in particular, Jarvis (1976). Figure 12 shows the results of a model run with the predicted cumulative totals of interception loss, transpiration and soil evaporation compared to the appropriate data. It is clear that the model performs adequately. A full and detailed discussion of the sensitivity of the predicted fluxes to changes in the model parameters and the results of the tests will be provided in Sellers and Dorman (in prep.).

5. SUMMARY AND FUTURE RESEARCH

The use of simple land-surface parameterizations in General Circulation Models (GCMs) of the atmosphere has shown that vegetation is an important factor influencing the exchanges of radiation, momentum and heat at the local scale and, by extension, the regional climate. To date, the parameterizations implemented within GCMs have consisted of either prescribed fields of albedo, momentum and moisture transfer coefficients or of simple conceptual models of the land surface. While these biophysically unrealistic models have indicated that the atmosphere is sensitive to the

condition of the land surface, they should not be relied on for any quantitative predictive experiments. Dickinson (1984) and Sellers et al. (1985) have attempted to incorporate biophysical principles into simple surface formulations appropriate for use within GCMs. The Simple Biosphere (SiB) model, described in this paper, is an attempt to design a scheme simple and robust enough to operate within the computing constraints of a GCM, yet not so simple as to be totally unrealistic in its representation of the biophysics of land surface-atmosphere interaction. So far, the model has only been tested against local micrometeorological observations, but it appears that its separate elements (radiation interception, turbulent transport, stomatal functioning, etc.) operate realistically and to within an acceptable accuracy. The model will be linked to a GCM for fully interactive studies in the near future. The model of Dickinson (1984), not discussed in this paper for reasons of brevity, has the same essential approach to the problem and is comparable in the design of many of its components. It is currently implemented within the Community Climate Model of the National Center for Atmospheric Research and is undergoing sensitivity tests.

The advantages of using a biophysically realistic model lies in the specification of measurable parameters and the output of physical state variables as part of the model prognostic calculations. There are two obvious areas where the specified or calculated fields of these quantities (as given by SiB or any comparable model) may be compared with remotely-sensed data obtained from satellite platforms for the purposes of model initialization and validation. First, we may compare the model initialization data set with narrow band visible (0.55 - 0.68 μm) and near infrared (0.73 - 1.1 μm) surface reflectance data as gathered by polar orbiting meteorological and earth observation satellites (see Tucker et al., 1985

and Tucker, 1978). It will be remembered that green leaves are highly absorbent in the visible wavelength interval and scatter strongly in the near-infrared. The Normalized Vegetation Index (NVI) of Tucker et al. (1985) is a dimensionless quantity that increases with chlorophyll density.

$$NVI = \frac{I_{n(NIR)} - I_{n(VIS)}}{I_{n(NIR)} + I_{n(VIS)}} \tag{58}$$

NVI = Normalized Vegetation Index

$I_{n(NIR)}$, $I_{n(VIS)}$ = nadir or near nadir surface reflectance in near infrared, visible wavelength intervals

The value of the NVI generally increases from ~ 0.2 for bare ground to 0.9 for a full green cover of vegetation. Tucker et al. (1985) have demonstrated the feasibility of producing global maps of the NVI using modest computer resources.

The NVI may be interpreted as an area-averaged photosynthetic capacity and hence related to a value of the minimum canopy resistance ($\overline{r_{st}}$ in the absence of stress factors) for continuous vegetative cover (see Sellers, 1985). The high temporal resolution of the meteorological satellite system makes feasible the use of such data for model initialization and validation.

Second, satellite data may be directly useful for the estimation of fields of surface temperature (equivalent to a combination of the SiB predicted prognostic variables of T_c and T_{gs}). From (54) and (56) it is clear that the air-surface temperature difference is proportional to the sensible heat flux and, if the surface net radiation is known, can be used to estimate the evapotranspiration rate. Thus, soil moisture storage could be inferred from a combination of satellite data, mesometeorological data and modeling. Susskind et al. (1984) and Carlson et al. (1984)

review current capabilities in the estimation of surface temperatures and regional evapotranspiration from satellite data. In the near future, microwave remote sensing (passive and active) may yield estimates of the surface soil moisture content and the vertical structure of the vegetation canopy (Schmugge, 1983).

In summary, little can be expected from unrealistic surface formulations in GCMs in the way of quantitative understanding of the interactions operating between the surface and the atmosphere. This understanding can only be achieved by biophysically-based models where the important features of the transfers of radiation, momentum and heat are described in a realistic fashion. Such an approach predicts physical state variables which can be compared with satellite data for the purposes of model initialization and validation.

ACKNOWLEDGEMENTS

Piers Sellers was a National Academy of Sciences/National Research Council Resident Research Associate during the period when this work was done. The author would like to extend his gratitude to the following researchers for useful discussions. Y. Mintz, Y. C. Sud, R. E. Dickinson, A. Dalcher, T. J. Schmugge, J. Shukla, R. J. Gurney, P. J. Camillo, B. J. Choudhury, V. V. Salomonson and C. J. Willmott. Special thanks go to J. Tippett and L. A. Wright for typing the manuscript. R. E. Dickinson is to be warmly thanked for his encouragement throughout this work and for providing considerable help with the radiative transfer component of SiB.

REFERENCES

Arakawa, A., 1972: Design of the UCLA general circulation model. Technical Report 7, Department of Meteorology, University of California, Los Angeles, U.S.A, 116 pp.

Calder, I. R., 1977: A model of transpiration and interception loss from a spruce forest in Plynlimon, Central Wales. J. Hydrol., 33, 247-265.

Camillo, P. J. and R. J. Gurney, 1985: A resistance parameter for bare soil evaporation models. Submitted to Soil Science.

Carlson, T., F. G. Rose and E. M. Perry, 1984: Regional scale estimates of soil moisture availability from GOES satellites. J. Agron., 16, 972-979.

Carson, D. J. and A. B. Sangster, 1981: The influence of land-surface albedo and soil moisture on general circulation model simulations. Numerical Experimentation Program Report No. 2, 5.14-5.21, Meteorological Office (U.K.), Bracknell, Surrey, U.K.

Carson, D. J., 1982: Current parameterizations of land surface processes in atmospheric general circulation models. In Land Surface Processes in Atmospheric General Circulation Models, P. S. Eagleson, editor, Cambridge University Press, Cambridge, U.K., 560 pp.

Charney, J. G., 1975: Dynamics of deserts and droughts in the Sahel. Quart. J. Roy. Met. Soc., 101, 193-202.

Charney, J. G., Quirk, W. J., Chow, S. H. and Kornefield, J., 1977: A comparative study of the effects of albedo change on drought in semi-arid regions. J. Atmos. Sci., 34, 1366-1385.

Clapp, R. B. and G. M. Hornberger, 1978: Empirical equations for some soil hydraulic properties. Water Resources Res., 14, 601-604.

Coakley, J. A., Jr. and P. Chylek, 1975: The two stream approximation in radiative transfer: Including the angle of incident radiation. J. Atmos. Sci., 32, 409-418.

de Laubenfels, D. J., 1975: World's vegetation: Formations and flora. Syracuse University Press, New York, U.S.A., 231 pp.

Dickinson, R. E., 1984: Modeling evapotranspiration for three-dimensional global climate models. 58-72, In Climate Processes and Climate Sensitivity, Geophys. Mon., 29, J. E. Hansen, editor.

Dickinson, R. E., 1983: Land surface processes and climate-surface albedos and energy balance. 305-353, In Advances in Geophysics, 25, Theory of Climate, B. Saltzman, editor.

Federer, C. A., 1979: A soil-plant-atmosphere model for transpiration and availability of soil water. Water Resources Res., 15, 555-562.

Garratt, J. R., 1978: Flux profile relations above tall vegetation. Quart. J. Roy. Met. Soc., 104, 199-211.

Goudriaan, J., 1977: Crop micrometeorology: A simulation study. Wageningen Center for Agricultural Publishing and Documentation. Wageningen, The Netherlands, 249 pp.

Gurney, R. J. and P. J. Camillo, 1984: Modeling daily evapotranspiration using remotely sensed data. J. Hydrol., 69, 305-324.

Hancock, N. H., P. J. Sellers and J. M. Crowther, 1983: Evaporation from a partially wet forest canopy. Annales Geophysicae, 1, (2), 139-146.

Jarvis, P. G., 1976: The interpretation of the variations in leaf water potential and stomatal conductance found in canopies in the field. Phil. Trans. Roy. Soc. Lond., B. 273, 593-610.

Kuchler, A. W., 1949: A physiognomic classification of vegetation. Ann. Assoc. Amer. Geogr., 39, 201-210.

Matthews, E., 1983: Global vegetation and land use: New high-resolution data bases for climate studies. Clim. Appl. Met., 22, 474-487.

Meador, W. E. and W. R. Weaver, 1980: Two-stream approximations to radiative transfer in planetary atmospheres: A unified description of existing methods and a new improvement. J. Atmos. Sci., 37, 630-643.

Milly, P. C. and P. S. Eagleson, 1982: Parameterization of moisture and heat fluxes across the land surface for use in atmospheric general circulation models. Report Number 279, Dept. of Engineering, Massachusetts Institute of Technology, Cambridge, MA 02139, 159 pp.

Mintz, Y., 1984: The sensitivity of numerically simulated climates to land-surface conditions. In: The Global Climate, J. Houghton, editor; Cambridge University Press, Cambridge/United Kingdom, 233 pp.

Monteith, J. L., 1973: Principles of environmental physics. Edward Arnold Ltd., London, 242 pp.

Monteith, J. L., G. Szeicz and P. E. Waggoner, 1965: The measurement and control of stomatal resistance in the field. J. Appl. Ecol., 2, 345-355.

Norman, J. M. and P. G. Jarvis, 1975: Photosynthesis in sitka spruce (picea sitchensis (bong.) carr.). V. Radiation penetration theory and a test case. J. Applied Ecology, 839-878.

Otterman, J., 1981: Plane with protrusions as an atmospheric boundary. J. Geophys. Res., 86, 6627-6630.

Paulson, C. A., 1970: Mathematical representation of wind speed and temperature profiles in the unstable atmospheric surface layer. Journ. Appl. Met., 9, 857-861.

Penman, H. L., 1948: Natural evaporation from open water, bare soil and grass. Proc. Roy. Soc. Lond., So. A., 193, 120-145.

Raupach, M. R. and A. S. Thom, 1981: Turbulence in and above plant canopies. Ann. Rev. Fluid Mech., 13, 97-129.

Ross, J., 1975: Radiative transfer in plant communities, 13-52. In Vegetation and the Atmosphere, 1, J. L. Monteith, editor, Academic Press, London.

Schmugge, T. J., 1983: Remote sensing of soil moisture: Recent advances. IEEE Trans., GE-21, 3, 336-344.

Sellers, P. J., 1981: Vegetation type and catchment water balance: A simulation study. Ph.D. Thesis, Leeds University, Department of Geography, 836 pp.

Sellers, P. J. and J. G. Lockwood, 1981: A computer simulation of the effects of differing crop types on the water balance of small catchments over long time periods. Quart. J. Roy. Met. Soc., 107, 395-414.

Sellers, P. J., 1985a: Canopy reflectance, photosynthesis and transpiration. Accepted by Int. J. Rem. Sens.

Sellers, P. J., 1985b: Modeling the effects of vegetation on climate. In: The geophysiology of the Amazon; Ed. R. E. Dickinson, publ. Wiley and Sons, London, N.Y.

Sellers, P. J., Y. Mintz and Y. C. Sud, 1985: A simple biosphere model (SiB) for use within general circulation models. Submitted to J. Atmos. Sci.

Shaw, R. H. and A. R. Pereira, 1982. "Aerodynamic roughness of a plant canopy: A numerical experiment. Agric. Met., 26, 51-65.

Shukla, J. and Y. Mintz, 1982: Influence of land-surface evapotranspiration on the Earth's climate. Science, 215, 1498-1501.

Shu Fen Sun, 1982: Moisture and heat transport in a soil layer forced by atmospheric conditions. M.Sc. Thesis, University of Connecticut, Connecticut, U.S.A., 72 pp.

Sud, Y. C. and W. E. Smith, 1985: The influence of surface roughness on the July circulation: A numerical study. Submitted to J. Atmos. Sci.

Sud, Y. C. and W. E. Smith, 1984: Ensemble formulation of surface fluxes and improvement in evapotranspiration and cloud parameterizations in a GCM. Bound. Layer Met., 29, 185-210.

Susskind, J., J. Rosenfield, D. Reuter and M. T. Chahine, 1984: Remote sensing of weather and climate parameters from HIRS2/MSU on TIROS-N. J. Geophys. Res., 89, 4677-4697.

Thom, A. S., 1971: Momentum absorption by vegetation. Quart. J. Roy. Met. Soc., 97, 414-428.

Tivy, J., 1977: Biogeography: A study of plants in the ecosystem. Publ. Oliver and Boyd, Edinburgh, Scotland, 3rd Edition, 374 pp.

Tucker, C. J., 1978: A comparison of satellite sensor bands for vegetation monitoring. Photogramm. Eng. Rem. Sens., 44, 11, 1369-1380.

Tucker, C. J., J. R. G. Townshend and T. E. Goff, 1985: African land-cover classification using satellite data. Science, 227, 369-375.

van der Honert, T. H., 1948: Water transport as a catenary process. Discuss. Faraday Soc., 3, 146-153.

van der Ploeg, R. R., G. Tassone and J. von Hoyningen-Heure, 1980: The joint measuring campaign 1979 in Ruthe (West Germany)-Description of preliminary data. Eur. Econ. Comm. Joint Res. Center, Ispra.

Walter, H., 1973: Vegetation of the earth. Publ. Heidelbeig Science Library, Springer-Verlag, N.Y., U.S.A., 237 pp.

Willmott, C. J., Klink, K., Legates, D., Rowe, C., 1984: Personal Communication.